A seven-year longitudinal study of the Alzheimer's disease blood metabolome

Bharadwaj Marella[1], Patrick Weinisch[1], Josef J. Bless[1], Shannon L. Risacher[2,3], Colette Blach[4], Naama Karu[5], Karel Kalecký[6], Tingting Wang[7,8], Kevin Huynh[7,8,9], Alexandra Kueider-Paisley[10], J. Will Thompson[11], Alzheimer's Disease Neuroimaging Initiative[+], Alzheimer's Disease Metabolomics Consortium[#], Teodoro Bottiglieri[6], Kwangsik Nho[2,3,12], P. Murali Doraiswamy[10,13], Andrew J. Saykin[2,3], Peter J. Meikle[7,8,9], Gabi Kastenmüller[1,*], Rima Kaddurah-Daouk[10,13,*], Matthias Arnold[1,10,*]

[1] Institute of Computational Biology, Helmholtz Zentrum München - German Research Center for Environmental Health, Neuherberg, Germany
[2] Department of Radiology and Imaging Sciences, Center for Neuroimaging, Indiana University School of Medicine, Indianapolis, Indiana, USA
[3] Indiana Alzheimer's Disease Research Center, Indiana University School of Medicine, Indianapolis, Indiana, USA
[4] Duke Molecular Physiology Institute, Duke University, Durham, NC, USA
[5] Tasmanian Independent Metabolomics and Analytical Chemistry Solutions (TIMACS), Hobart, Tasmania, Australia
[6] Center of Metabolomics, Institute of Metabolic Disease, Baylor Scott and White Research Institute, Dallas, TX, USA
[7] Baker Heart and Diabetes Institute, Melbourne, Australia
[8] Baker Department of Cardiometabolic Health, University of Melbourne, Victoria, Australia.
[9] Department of Cardiovascular Research Translation and Implementation, La Trobe University, Melbourne, Australia
[10] Department of Psychiatry and Behavioral Sciences, Duke University, Durham, NC, USA
[11] Move Analytical, Carrboro, NC, USA
[12] Center for Computational Biology and Bioinformatics, Indiana University School of Medicine, Indianapolis, IN, USA
[13] Department of Medicine, Duke Center for the Study of Aging and Duke Institute for Brain Sciences, Duke University School of Medicine, Durham, NC, Durham

[*] Correspondence to: g.kastenmueller@helmholtz-muenchen.de, rima.kaddurahdaouk@duke.edu, and matthias.arnold@helmholtz-muenchen.de

[+] Data used in preparation of this article were obtained from the Alzheimer's Disease Neuroimaging Initiative (ADNI) database (adni.loni.usc.edu). As such, the investigators within the ADNI contributed to the design and implementation of ADNI and/or provided data but did not participate in analysis or writing of this report. A complete listing of ADNI investigators can be found at: http://adni.loni.usc.edu/wp-content/uploads/how_to_apply/ADNI_Acknowledgement_List.pdf

[#] Metabolomics data used in preparation of this article were generated by the Alzheimer's Disease Metabolomics Consortium (ADMC). As such, the investigators within the ADMC provided data but did not participate in analysis or writing of this report. A complete listing of ADMC investigators can be found at: https://sites.duke.edu/adnimetab/team/

Abstract

Metabolic dysregulation is a hallmark of Alzheimer's disease (AD), yet the temporal nature of metabolite–phenotype associations remains poorly understood. We systematically evaluated 506 serum metabolites across 4,063 longitudinal samples from 1,430 participants in the Alzheimer's Disease Neuroimaging Initiative (ADNI), applying cross-sectional single-timepoint analyses, multi-timepoint meta-analysis, and time-interaction analysis. Across 15 AD-related phenotypes, we identified 311 metabolites to be significantly associated with disease. Of those, 281 emerged from the multi-timepoint meta-analysis, 243 (216 overlapping/27 additional) from cross-sectional analyses, and 19 (16 overlapping/3 additional) metabolites that showed a significant evolution of their association with AD over time. In total, 128 metabolites (41%) showed persistent associations over time, providing evidence for chronic and systemic metabolic dysregulation in the disease. This, together with the comparably small number of metabolites showing evolving changes, suggests that many metabolic alterations in AD do not change substantially anymore once they manifested. Our findings confirm impaired fatty acid and energy metabolism, disrupted neurotransmitter systems, and oxidative stress as key metabolic features of AD. We demonstrate broad replication of the reported metabolite associations in prior studies and an independent lipidomics dataset in ADNI. In summary, this work expands previous metabolomics studies in AD and provides novel leads regarding timing and persistence of metabolic alterations across the disease trajectory.

1. Introduction

Alzheimer's disease (AD) is characterized by the accumulation of amyloid-beta peptides in plaques and hyperphosphorylated tau protein in neurofibrillary tangles in the brain, particularly in the medial temporal lobe [1]. Further hallmarks of the disease are deregulated glucose uptake, impaired cholesterol transport via Apolipoprotein E, and neuroinflammation, together leading to neurodegeneration and ultimately dementia.

Previous studies have demonstrated that multiple metabolic pathways are altered during the onset and progression of AD, highlighting disruptions in lipid metabolism, amino acid catabolism, energy pathways, neurotransmission, and oxidative stress response, among others. For example, Trushina et al. [2] identified early alterations in mitochondrial and lipid metabolism in both plasma and cerebrospinal fluid (CSF) of individuals with mild cognitive impairment (MCI), a prodromal stage of AD. Han et al. [3] demonstrated alterations in sphingolipid and sterol metabolism linked to cognitive decline. Toledo et al. [4] showed that changes in various metabolic pathways, particularly those involving acylcarnitines, sphingomyelins, and phosphatidylcholines, are associated with AD pathological progression and clinical outcomes. Results from a study by MahmoudianDehkordi et al. [5] suggests that the gut-brain axis may contribute to AD through altered bile acid metabolism. More recently, Ambeskovic et al. [6] found levels of several metabolites, including N-acetylaspartate, gamma Aminobutyric acid (GABA), and leucine, to be increased in the hippocampus of post-mortem human brain samples when comparing AD to non-AD control subjects. In contrast, Batra et al. [7] showed that GABA levels in the dorsolateral prefrontal cortex are negatively associated with AD traits, highlighting region-specific metabolite-level differences as crucial for disease progression. Another study examining plasma metabolic profiles found that 18 plasma metabolites (including amino acids, lysophosphatidylcholines, phosphatidylcholines, and sphingolipids) were able to predict future dementia risk [8]. In addition, the neurotransmitter system has been shown to be affected in AD (for a review, see [9]). For example, higher concentrations of the neurotransmitter noradrenaline in plasma of AD patients has been found to be associated with the higher levels of soluble amyloid plaques in CSF, which is interpreted as reflecting fewer brain plaques, and higher cognition scores [10]. Finally, recent metabolomics studies have suggested the role of oxidative stress in AD: Knörnschild et al. [11] reported disrupted glucose oxidation and elevated oxidative stress metabolites (e.g., L-cysteine,) in AD mouse models, while Ahmad et al. [12] demonstrated strong associations between CSF isoprostanes and tau pathology in MCI patients, and Batra et al. [7] showed disruptions of the glutathione pathway among others, further highlighting oxidative imbalance as a possible driver of neurodegeneration. Cortisol, which is implicated in oxidative stress among other metabolic pathways, has been suggested as a relevant signaling hormone in AD. In a cross-sectional study, Dronse et al. [13] found that elevated morning serum levels of cortisol correlated with poorer verbal memory in AD patients compared to healthy controls. Furthermore, Mosconi et al. [14] found that higher serum cortisol was linked to lower total brain volume, reduced glucose metabolism in the frontal cortex and increased amyloid-ß burden in regions vulnerable to AD, with these effects showing sex-specific patterns.

While by now there is an increasingly large body of consistent links between AD and metabolic dysregulation, there are also some contradictory findings. Instances include, among others, the amino acid lysine and ceramides: Although decreased lysine has been observed in post mortem

tissue in the hippocampus [15] and plasma samples of AD patients compared to controls [16], elevated lysine levels have been found in post mortem tissue in the dorsolateral prefrontal cortex (DLPFC) [7] and in urine samples of AD patients [17], pointing to complex metabolic dynamics across tissues and brain regions. Similarly, ceramide levels in plasma were shown to be lower at baseline in patients with mild cognitive impairment (MCI) compared to cognitively normal individuals and AD patients, whereas higher levels were predictive of greater cognitive decline and greater hippocampal atrophy in MCI patients, suggesting a dynamic evolution of metabolic changes across disease stages [18].

Every individual exhibits distinctive metabolic signatures, and shifts in metabolite levels can reflect disease states and underlying molecular mechanisms. This can be particularly informative in complex, progressive diseases such as AD. While traditional cross-sectional metabolomics captures inter-individual differences at a single time point, it is limited in its ability to track intra-individual changes over time. Longitudinal metabolomics, which involves repeated measurements from the same individuals, enables the study of temporal trajectories of metabolites across disease progression. This dynamic insight is especially important in the prodromal stage of AD, when subtle metabolic alterations may precede clinical symptoms, and the contribution of biological pathways may shift as disease advances. Notably, Huang et al. [19] observed changes in metabolic pathways (e.g. glutathione metabolism, tryptophan metabolism, bile acid metabolism) in older individuals with physio-cognitive decline compared to normal aging controls. Furthermore, comparing cross-sectional and longitudinal data permits assessment of the temporal robustness of metabolite–phenotype associations (see Lawrence et al. [20]).

In this study, we utilized data from the Alzheimer's Disease Neuroimaging Initiative (ADNI) study, a longitudinal cohort that provides detailed measurements of disease phenotypes, including AD biomarkers in CSF, neurocognitive performance, and neuroimaging markers of neuropathology and -degeneration, alongside blood-based longitudinal metabolite profiles generated by the AD metabolomics consortium. ADNI collected data every 6 to 12 months, offering a valuable foundation for assessing the robustness and consistency of associations between blood metabolites and AD onset, severity, and progression. In our prior work in ADNI, we found that individuals who progressed to AD showed a significant 3–4.8% reduction in ether lipid species compared to non-converting controls and those with MCI [21]. Building on these findings, we expanded our investigation to include polar metabolites and adopted a broader analytical approach to evaluate the reproducibility of such associations.

To achieve this, we contrasted metabolic alterations in AD observed in cross-sectional and longitudinal analyses. More specifically, we conducted cross-sectional analyses to identify metabolic differences in AD at single time points, complemented by two types of longitudinal analyses: a multi-timepoint meta-analysis examining the persistence of metabolic differences; and a time-interaction model to identify metabolites that show a changing relationship to the disease over time. By combining the results from these analyses, we then categorized metabolites by their association patterns with disease, highlighting those that are most consistently linked to AD or are continuing to change along the disease trajectory. Our findings provide a first reference to prioritize metabolic pathways not only cross-sectionally, but longitudinally, allowing for a better understanding of metabolic disruptions in AD and a more solid basis for potential novel, metabolically-guided therapeutic strategies.

2. Methods

2.1. Study population and diagnostic classification

Data used in the preparation of this article were obtained from the Alzheimer's Disease Neuroimaging Initiative (ADNI) database (adni.loni.usc.edu). The ADNI was launched in 2003 as a public-private partnership, led by Principal Investigator Michael W. Weiner, MD. The primary goal of ADNI has been to determine whether serial magnetic resonance imaging (MRI), positron emission tomography (PET), biological markers, and clinical and neuropsychological assessments can be combined to measure the progression of mild cognitive impairment (MCI) and early Alzheimer's disease (AD). For up-to-date information, see www.adni-info.org. Written informed consent was obtained at enrollment, which included permission for analysis and data sharing. Consent forms were approved by each participating site's institutional review board.

The definition of probable AD in ADNI followed the NINDS-ADRDA criteria. Specifically, individuals with Mini-Mental State Exam (MMSE) scores between 20 and 26 (inclusive) and a Clinical Dementia Rating Scale (CDR) of 0.5 or 1.0 were classified as patients with mild AD and were followed up for a maximum of 2 years into the study [22]. Participants were defined as MCI if they had MMSE scores between 24 and 30, a subjective memory complaint, objective memory loss measured by education-adjusted scores on Wechsler Memory Scale Logical Memory II, a CDR of 0.5, absence of significant levels of impairment in other cognitive domains, and essentially preserved activities of daily living [23].

In this study, we leveraged data from 1524 ADNI-1, -GO, and -2 participants. Clinical data and biological samples were collected at baseline and every 6-12 months for a maximum of 10 years (maximum number of visits = 13). To group participants into a general longitudinally valid diagnostic group, we screened the diagnoses reported for each individual across all visits where metabolomics data was available, resulting in five longitudinal diagnostic classifications: cognitively normal (CN; *n*=383), stable MCI (*n*=423), MCI converters (CN to MCI; *n*=66), AD converters (CN or MCI to AD; *n*=294), reflecting progression to AD dementia at any time point during the course of the study, and AD (*n*=264). Individuals exhibiting atypical diagnostic trajectories—such as reversion from MCI or AD to CN, or fluctuation between stages—were excluded from this classification to ensure consistency in group assignment (*n*=72). As an additional outcome variable, the diagnostic status recorded at each visit was numerically encoded as CN = 0, MCI = 1, and AD = 2 to capture time-resolved diagnostic trajectories for all participants.

2.2. Phenotypic assessments

The available quantitative longitudinal outcomes included: (1) concentrations of amyloid-beta ($A\beta_{1-42}$) and tau (phosphorylated (p-)tau and total (t-)tau) in CSF, (2) measures of neurodegeneration (glucose uptake measured by Fluorodeoxyglucose-Positron Emission Tomography (FDG-PET), grey matter volume and thickness, entorhinal volume and thickness, and hippocampal volume), and (3) neurocognitive scores (cognition subscale of the 13-item AD assessment scale - ADAS-Cog. 13, ADNI composite scores on memory, executive function, visospatial functioning and language). In total, fifteen clinical phenotypes and diagnostic group comparisons were selected for association analysis, representing diverse readouts that capture

various aspects of AD. These phenotypes were defined based on the ATN framework [24]—which classifies AD by amyloid, tau, and neurodegeneration biomarkers—and were extended to include cognitive assessments and diagnostic status. Comprehensive descriptions of these phenotypes and their transformations, along with the corresponding covariates specific to each phenotype, are provided in **Supplementary Table S1**.

$A\beta_{1\text{-}42}$, t-tau, and p-tau_{181p} in CSF samples were measured via a fully automated Roche Elecsys immunoassay applying a sample preparation procedure with two incubation steps [25, 26].

MRI protocol and data were accessed through LONI (https://adni.loni.usc.edu/). In brief, MRI imaging was acquired using a 1.5 T or 3 T MRI scanner with the sequences of T1 and dual echo T2-weighted imaging (ADNI-1), or a 3 T MRI scanner with fully sampled and accelerated T1-weighted imaging in addition to 2D FLAIR and T2*-weighted imaging (ADNI-GO/2). To process MRI scans and extract whole brain and ROI (region of interest)-based neuroimaging measurements determined by automated segmentation and parcellation including volumes and cortical thickness, we used FreeSurfer V6 (https://surfer.nmr.mgh.harvard.edu/fswiki) [27-29]. After the cortical surface was reconstructed, the cortical thickness at each vertex was calculated by taking the Euclidean distance between the grey/white boundary and the grey/CSF boundary at each vertex on the surface.

For FDG-PET, we used a ROI–based measure representing the average glucose uptake across the left and right angular gyrus, left and right temporal lobes, and bilateral posterior cingulate cortex. These values were derived from preprocessed scans (including co-registration, averaging, spatial standardization, and resolution harmonization) and intensity-normalized using a pons region to calculate standard uptake value ratio (SUVR) means [30, 31].

2.3. Metabolomics profiling and data preprocessing

Serum metabolites were quantified using the MXP® Quant 500 platform (Biocrates Life Sciences AG), a targeted, kit-based metabolomics assay. Sample preparation and metabolomics profiling were conducted by the Alzheimer's Disease Metabolomics Consortium at Duke University using 10 µL aliquots resulting in 624 metabolites belonging to 26 biochemical classes. All procedures, including sample extraction, metabolite detection, identification, quantification, and initial quality control (QC), were performed in accordance with standardized protocols [4, 32]. In addition to individual metabolite measurements, the dataset included vendor-defined biologically relevant sums and ratios reflecting functions such as enzyme activity. These composite measures (from the MetaboINDICATOR™ software) were derived from raw concentrations and processed in the same manner as single metabolites. Furthermore, we have aggregated metabolites from the 26 biochemical classes into 11 categories to enhance the comprehension of the associations observed across the various classes (see **Supplementary Table S2**)

A comprehensive quality control procedure was applied to exclude unreliably measured metabolites from the dataset. First, 98 metabolites were removed due to having greater than 30% missingness in at least one cohort (ADNI-1 and ADNI-GO/2 were profiled in two separate runs). Next, an additional 8 metabolites were excluded based on a coefficient of variation (CV) exceeding 30% in quality control reference materials. A further 12 metabolites were removed due to complete missingness across one or more assay plates. In total, 118 metabolites were removed from further analysis. Details of the quality control assessments are provided in **Supplementary Table S3**).

The resulting dataset comprised 506 metabolites across 26 biochemical classes and 4,884 samples from 1,524 subjects. Biological replicates were averaged (n=41), and samples with more than 30% missing data were excluded (n=10). Multivariate outlier detection using Mahalanobis distance identified outliers with $D^2 > 1.5 \times \max(D^2_{expected})$, leading to the exclusion of 168 samples (6 subjects). Following $\log_2$ transformation and removal of 284 non-fasting samples (15 subjects), missing metabolite values were imputed using random forest–based imputation [33]. Subjects with atypical diagnostic trajectories were removed (subjects = 72; samples = 270). The final three timepoints (48 samples) were excluded to minimize bias. After all filtering steps, the final dataset included 4,063 samples from 1,430 subjects, with approximately 80% of samples collected at baseline, 12 months, and 24 months (hereafter referred to as three main timepoints). The decision to limit timepoints to a maximum of 24 months here was further based on the fact that participants who entered the ADNI studies with mild AD at baseline per study protocol dropped out after 24 months.

2.4. Identification of significant medication effects

To account for the influence of medications on the metabolome, we employed the Boruta feature selection algorithm [34, 35]. The procedure was iterated 100 times to refine the set of selected and rejected features, and those exceeding 4 standard deviations above the mean importance were retained as covariates in subsequent regression models. A total of 41 and 21 significant medication–metabolite associations were identified at baseline and longitudinally at the three main timepoints, respectively. Several of these medications are commonly used in the treatment of Alzheimer's disease, although AD-specific anti-dementia drugs were excluded from the analysis (**Supplementary Figure S1; Supplementary Tables S4** and **S5**).

2.5. Statistical analysis

Single-timepoint cross-sectional analyses were performed to examine associations between metabolite levels and disease phenotypes at each of the three main timepoints. In parallel, two mixed-effects models for repeated measures (MMRMs) were employed to assess metabolite–phenotype associations longitudinally. The first model incorporated the three main timepoints, with subject and time specified as random effects (except for time-resolved diagnostic status, where we used time as a fixed effect), to evaluate the consistency of associations across time (multi-timepoint meta-analysis). The second model included all timepoints, subjects as a random effect, and a time-by-phenotype interaction term to assess temporal variation in associations (time-interaction analysis). To check for potential bias from the additional timepoints, we conducted a sensitivity analysis using only the three main timepoints as well. We further performed paired *t*-tests, as an additional line of evidence, in individuals who transitioned from CN to MCI or from MCI to AD within six to twelve months, with analyses restricted to transitions involving ≥30 individuals to ensure adequate power. To rule out spurious associations from imputation, we performed another sensitivity analysis on non-imputed data (**Supplementary Table S6**).

All regression models were adjusted for sex, age, education, BMI, APOE ε4 status, relevant medications, and phenotype-specific covariates (see section 2.2 and **Supplementary Table S1**).

For lipids, we further included log_2-transformed levels of total cholesterol and HDL cholesterol as covariates.

For replication of lipid associations, we performed identical analyses on lipid species also available in independently generated lipidomics data [21] from a largely overlapping set of longitudinal ADNI samples. For this, we first mapped lipid species with significant associations from the MXP® Quant 500 platform to the lipidomics dataset. Given the greater analytical resolution of the lipidomics platform compared to the MXP® Quant 500, e.g. for phosphatidylcholines, and the ambiguity of triglyceride annotations in both platforms, this resulted in several 1:n mappings (see **Supplementary Table S7**). Consequently, replication was defined as follows: if any lipid species in the lipidomics dataset that mapped to a given lipid from the MXP® Quant 500 platform demonstrated a significant association with AD in the same direction, the corresponding lipid in the MXP® Quant 500 platform was considered replicated.

The Li and Ji method [36] was used for multiple hypothesis testing correction, which in a Bonferroni-like fashion adjusts for the effective number of independent metabolic features among the 506 metabolites at baseline (n=122 independent features). A similar correction method was applied to the replication analysis in the lipidomics dataset, where we adjusted for 120 unique lipid species that could be mapped to significant lipids from the MXP® Quant 500 (n= 35 independent features).

Beyond single metabolite tests, we conducted p-gain analysis [37] to assess whether associations were driven primarily by individual metabolites or by informative sums and ratios (see Section 2.3).

3. Results

3.1. Cohort characteristics

In this study, we leveraged longitudinal metabolomics data generated on 4063 blood samples as well as longitudinal phenotypic data from 1430 participants of the ADNI-1, -GO and -2 cohorts. 1293 participants had metabolomics data available starting at baseline (**Table 1**). Blood samples were collected at annual or biannual follow-ups after study enrollment, spanning a total of 10 time points and seven years, respectively (**Figure 1**). The majority of the data (approximately 80%) was concentrated at three main timepoints: baseline, 12 months, and 24 months.

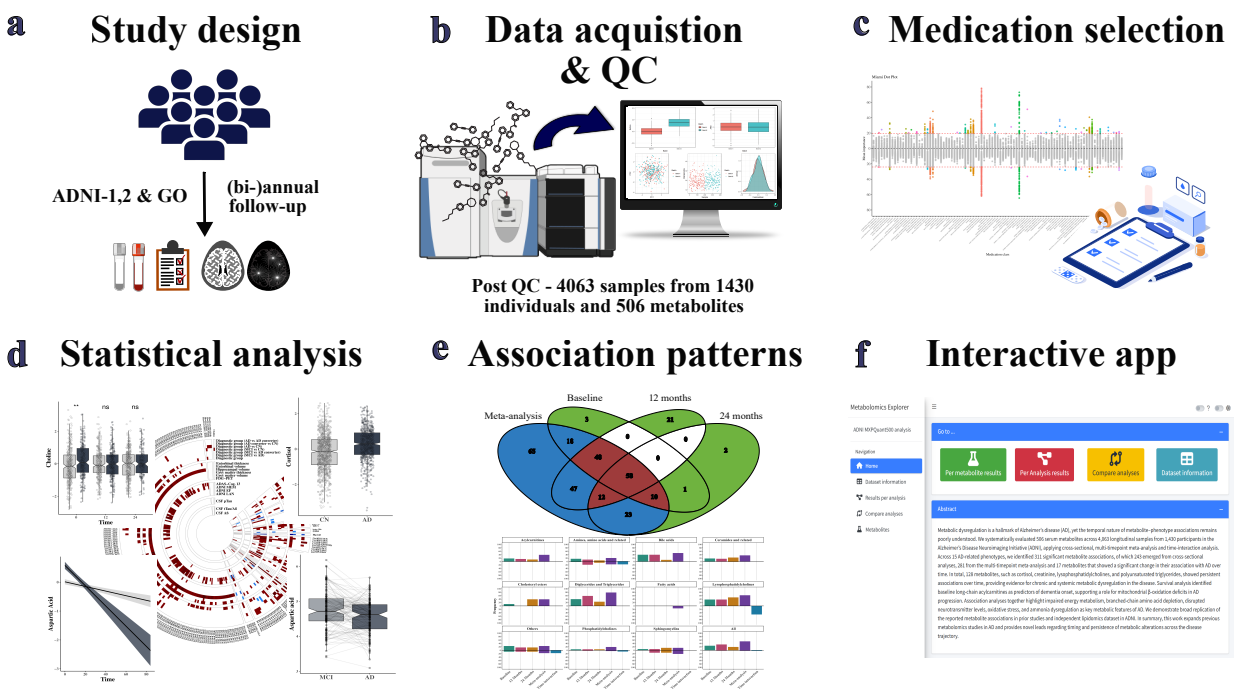

Figure 1: Analysis workflow. (a) Participants from the ADNI-1, -GO, & -2 studies were followed up annually or biannually, and blood and CSF samples were collected along with cognitive assessments and neuroimaging. **(b)** Metabolite concentrations were measured on the MXP® Quant 500 platform. After rigorous quality control, the final dataset consisted of 4,063 samples from 1,430 participants. **(c)** Feature selection analysis was performed using boruta backward random forest method to identify medications that are associated with metabolite levels and later used as covariates in downstream analyses. **(d)** The different types of statistical analyses conducted in this study, covering cross-sectional single timepoint analysis, multi-timepoint meta-analysis and time-interaction analysis. **(e)** Assessing persistence of associations observed and identifying the patterns of associations found for the different metabolites investigated in this study. **(f)** All study outcomes are available through an interactive web application at https://metabolomics.helmholtz-munich.de/mxtra_ad/.

Variable	Overall N = 1,430[1]	CN N = 383[1]	CN-MCI converter N = 66[1]	MCI stable N = 423[1]	AD converter N = 294[1]	AD N = 264[1]	p-value[2]
Age	76 ± 7	76 ± 6	80 ± 6	75 ± 8	76 ± 7	75 ± 8	**<0.001**
BMI	26.6 ± 4.7	26.9 ± 4.8	26.4 ± 4.8	27.1 ± 4.8	26.2 ± 4.6	25.8 ± 4.4	**<0.001**
Total cholesterol	2.29 ± 0.08	2.29 ± 0.07	2.26 ± 0.08	2.29 ± 0.08	2.29 ± 0.08	2.29 ± 0.08	0.2
HDL cholesterol	0.58 ± 0.11	0.59 ± 0.11	0.58 ± 0.14	0.57 ± 0.11	0.58 ± 0.11	0.58 ± 0.11	0.2
Sex							**0.002**
Female	638 (45%)	204 (53%)	27 (41%)	177 (42%)	116 (39%)	114 (43%)	
Male	792 (55%)	179 (47%)	39 (59%)	246 (58%)	178 (61%)	150 (57%)	
APOE ε4							**<0.001**
-	762 (53%)	281 (73%)	46 (70%)	248 (59%)	101 (34%)	86 (33%)	
+	668 (47%)	102 (27%)	20 (30%)	175 (41%)	193 (66%)	178 (67%)	

[1] Mean ± SD; n (%)
[2] Kruskal-Wallis rank sum test; Pearson's Chi-squared test

Table 1: Characteristics of the study cohort. Levels of high-density lipoprotein (HDL) cholesterol and total cholesterol are log_2-transformed and limited to baseline. *CN – cognitively normal controls; MCI – participants with mild cognitive impairment; AD – participants with clinical Alzheimer's disease; CN-MCI converter - CN to MCI converters; AD converters - CN or MCI to AD converters; BMI - body mass index.*

3.2 Identification of persistent, latent, and episodic associations

We first conducted cross-sectional analyses to identify serum metabolites associated with disease phenotypes at each of the three main timepoints separately. We obtained 138 significant associations (at a Bonferroni-adjusted $p < 4.1 \times 10^{-4}$) at baseline, 186 significant associations at 12 months, and 106 significant associations at 24 months, totaling to 243 unique metabolites (48.02%) that were significant in at least one analysis (**Supplementary Table S8; Supplementary Figure S4**). Cortisol was the metabolite associated with the largest number of phenotypes at baseline and at 24 months. At 12 months, triglyceride (TG) (18:1/34:4) showed the highest number of phenotype associations. Associated metabolites covered 10 of the 26 metabolite classes assessed here at baseline and 24 months, and 9 classes at 12 months (**Supplementary Table S9**). Among the tested phenotypes, hippocampal volume (n=98 associations) showed the highest number of associations at baseline, and ADAS-Cog. 13 at 12 months (n=119) and 24 months (n=70) **(Supplementary table S10).**

Next, on top of the cross-sectional analyses, we employed a multi-timepoint meta-analysis that incorporated the three main timepoints simultaneously, modeling time and subject as random effect variables to test the persistence of associations and their effect directions over time. Here, we discovered 281 out of 506 metabolites (55.53%) with significant associations. The majority of metabolites (94.31%) showed higher levels with more advanced disease phenotypes and diagnostic status, while 15 metabolites showed negative associations. This was consistent with our observations in the single timepoint cross-sectional analyses (**Figure 2; Supplementary Figure S4**). Cortisol was the metabolite associated with the largest number of phenotypes in the meta-analysis. Overall, metabolites from 20 of the 26 metabolite classes were associated with disease phenotypes in this meta-analysis, with triglycerides being the most frequently associated in absolute numbers, and fatty acids the least **(Supplementary Table S9).** Among the tested phenotypes, hippocampal volume (n=203 associations), ADAS-Cog 13 score (n=109), and the composite memory score (n=129) exhibited the largest number of significant metabolite associations in the multi-timepoint meta-analysis **(Supplementary Table S10).**

We then categorized all significant metabolite–AD associations based on their recurrence across phenotypic endpoints and the two models (**Figure 3** and **Supplementary Table S11**). Metabolites showing consistent cross-sectional associations at two or more single-timepoint analyses plus were also significant in the multi-timepoint meta-analysis were classified as persistently associated metabolites (*n*=128). Those cross-sectionally significant at none or just one single timepoint but also in the multi-timepoint meta-analysis were categorized as latent (*n*=153), where significant signals only emerge with large statistical power available. The third category, episodic metabolites (*n*=27), included metabolites that were significant only in single-timepoint cross-sectional analyses but not in the multi-timepoint meta-analysis, indicating weak or transient effects. Out of those, 26 were only detected at one single timepoint.

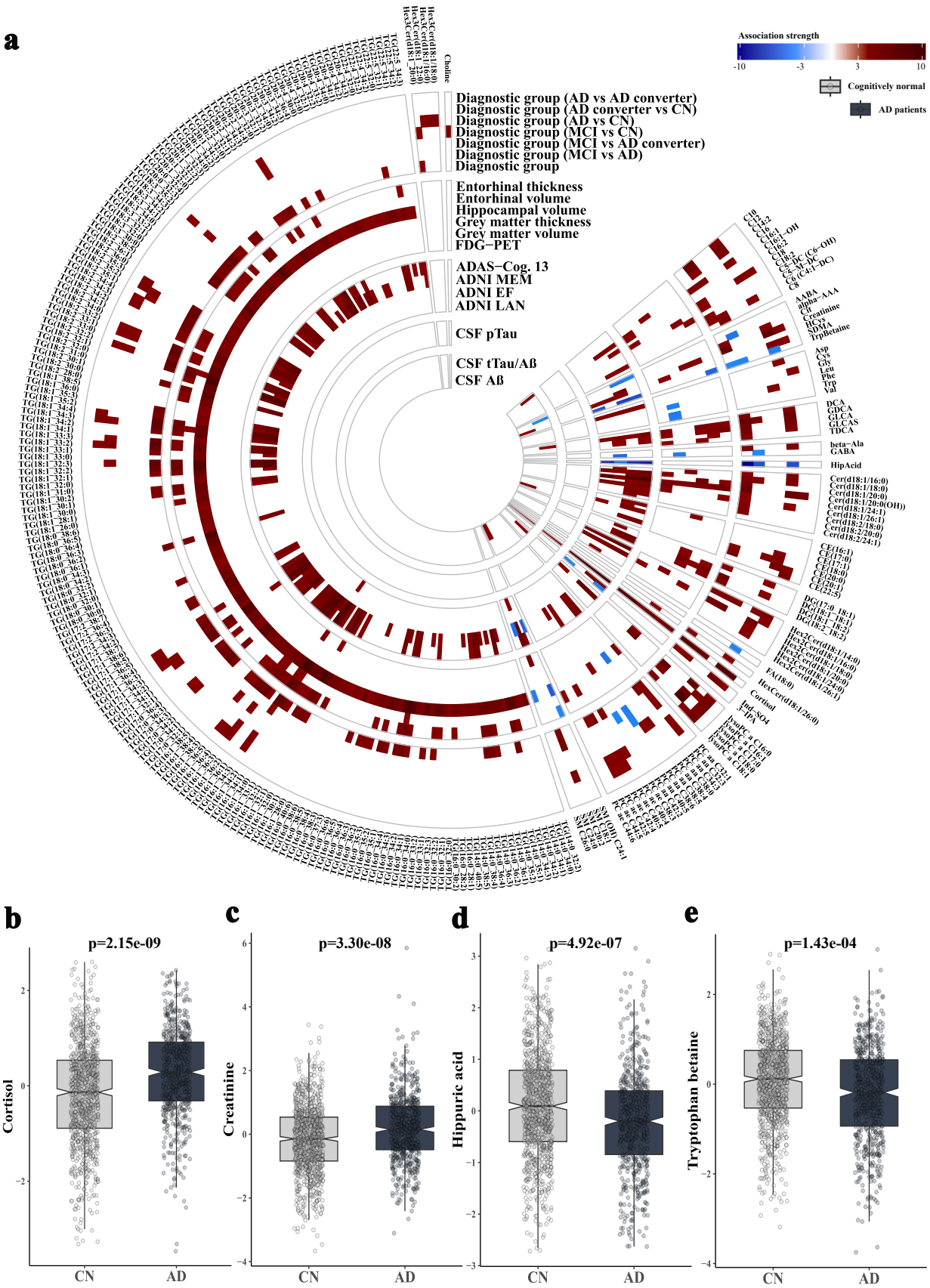
a
Association strength
-10
-3
3
10
Cognitively normal
AD patients
Diagnostic group (AD vs AD converter)
Diagnostic group (AD converter vs CN)
Diagnostic group (AD vs CN)
Diagnostic group (MCI vs CN)
Diagnostic group (MCI vs AD converter)
Diagnostic group (MCI vs AD)
Diagnostic group
Entorhinal thickness
Entorhinal volume
Hippocampal volume
Grey matter thickness
Grey matter volume
FDG−PET
ADAS−Cog. 13
ADNI MEM
ADNI EF
ADNI LAN
CSF pTau
CSF tTau/Aß
CSF Aß
Choline
b
p=2.15e-09
Cortisol
CN
AD
c
p=3.30e-08
Creatinine
CN
AD
d
p=4.92e-07
Hippuric acid
CN
AD
e
p=1.43e-04
Tryptophan betaine
CN
AD

Figure 2: Significant associations in multi-timepoint meta-analysis. (a) Circular heatmap showing all significant associations obtained. Each individual track represents a particular phenotype, red color constitutes positive association, and blue color represents negative associations. Association strength is calculated as $-\log_{10}(p)\cdot\text{sign}(\beta)$ where p is the p-value associated with the disease phenotype and β is its estimated effect coefficient. All effect directions across phenotypes were aligned so that positive beta estimates consistently reflect correlation with worse disease outcome. Metabolites are grouped by the biochemical classes provided by the platform vendor. **(b-e)** Exemplary boxplots displaying whitened residual values extracted from the multi-timepoint meta-analysis model in controls and AD patients, respectively, for the two most significant positive (cortisol, creatinine) and negative (hippuric acid, tryptophan betaine) associations with AD. Box plots display the median (central line), interquartile range (box bounds), whiskers extending to the smallest and largest values within 1.5 times the interquartile range from the quartiles, and notches indicating the 95% confidence interval for the median. All tests were two-sided and raw *p* values were reported. Source data are provided as a Source Data file. *CN – cognitively normal controls; AD – participants with clinical Alzheimer's disease.*

The majority of the 128 persistent metabolites were TGs and diglycerides (DGs) (*n* = 95). The rest of the metabolites included: cortisol, creatinine, symmetric dimethylarginine (SDMA), alpha-amino adipic acid (α-AAA), choline, phenylalanine, alanine, tryptophan betaine, indoxyl sulphate, hippuric acid, decanoylcarnitine (C10:0), dodecanoylcarnitine (C12:0), octadecanoylcarnitine (C8:0), cholesteryl esters (CE) 20:1 and CE(22:5), the glycine-conjugated secondary bile acids glycodeoxycholic acid (GDCA), glycolithocholic acid (GLCA) and GLCA sulfate (GLCAS), phosphatidylcholine (PC) aa C32:3, sphingomyelin (SM) C20:2, hydroxy-SM C24:1, lyso-PCs (LPC) C16:0, C16:1, and C18:0, and nine (hexosyl-)ceramides. Of the 153 metabolites in the latent category, the majority were again TGs and DGs (n=93). The other metabolites included: aspartic acid, citrate, cysteine, α-aminobutyric acid (AABA) and γ-aminobutyric acid (GABA), homocysteine, glycine, leucine, valine, tryptophan, deoxycholic acid (DCA), taurodeoxycholic acid (TDCA), fatty acid (FA) C18:0, 3-indole-proponoic acid, LPCs C17:0 and C18:1, SMs C18:1, C24:0, and C26:0, five cholesteryl esters, ten acylcarnitines, eleven (hydroxyl-)ceramides, and 15 PCs. Lastly, the 27 metabolites in the episodic category included: 3-methylhistidine, serine, lysine, isoleucine, sarcosine, hydroxy-SM C22:1, dihydroceramide (d18:0/24:0), dihexosylceramide (d18:1/22:0), trihexosylceramide (d18:1/24:1), six PCs and twelve TGs/DGs.

To further substantiate the temporal classification of metabolites, we performed replication analysis using an independent lipidomics dataset generated on largely overlapping ADNI samples (**Supplementary Tables S12–S14** and **Supplementary Figure S2**) and compared results across platforms. Out of 265 lipids showing significant associations, 189 could be mapped to 120 unique corresponding lipid species in the lipidomics dataset (**Supplementary Table S7**). Of these 189 lipids, 129 (68.25%; n=81 unique lipids) could be successfully replicated. Specifically, 69 lipids were classified as persistent, of which 59 (85.51%) were replicated; 105 were classified as latent, of which 69 (65.71%) were replicated; and 5 were classified as episodic, of which 1 (20%) were replicated, supporting the proposed temporal classification by reproducibility based on replication success.

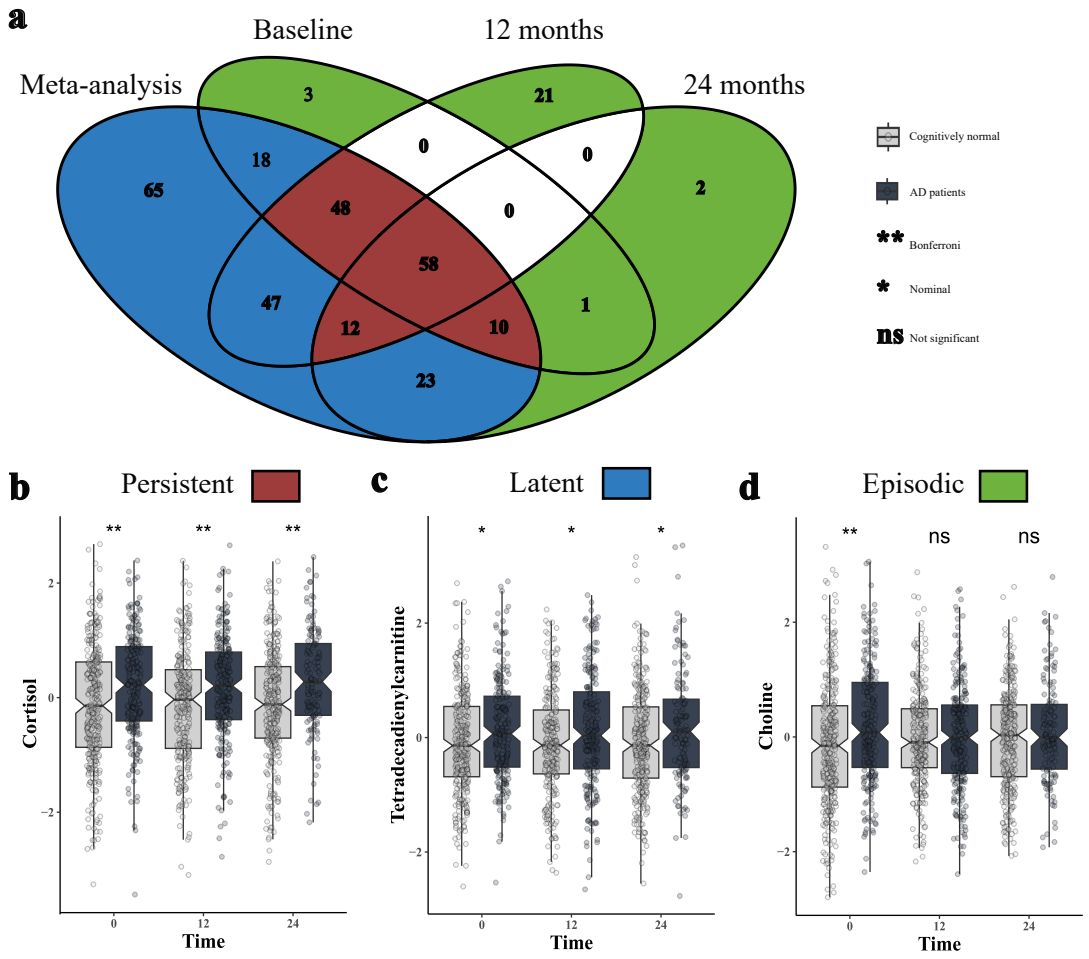

Figure 3: Temporal patterns of associations. (a) Venn diagram visualizing the shared significant metabolites across single timepoint cross-sectional analysis and the multi-timepoint meta-analysis. The Venn diagram is colored according to the respective categories, which are defined as follows: (i) Persistent metabolites (n=128): Significant in the multi-timepoint meta-analysis and in all or ≥2 single-timepoint analyses. (ii) Latent metabolites (n=153): Significant in the multi-timepoint meta-analysis but in ≤1 single-timepoint analysis. (iii) Episodic metabolites (n=27): Significant in one or more single-timepoint analyses but not in the meta-analysis. **(b-d)** Examples for the association patterns observed across the different models that define the different categories. The y-axis displays metabolite residuals derived from single time point models, while the x-axis represents time in months. Residuals are stratified by diagnostic groups (CN and AD), p-value significance is reported as calculated in the single time point cross-sectional analyses. Box plots display the median (central line), interquartile range (box bounds), whiskers extending to the smallest and largest values within 1.5 times the interquartile range from the quartiles, and notches indicating the 95% confidence interval for the median. All tests were two-sided and raw *p* values were reported. Source data are provided as a Source Data file. *CN – cognitively normal controls; AD – participants with clinical Alzheimer's disease.*

3.3. Identification of evolving metabolic changes over time

In the time-interaction analysis, we extended this framework by including time-by-phenotype as an interaction term, allowing effect sizes to vary across time and thus capturing whether the

strength or effect direction of associations changed longitudinally (**Figure 4**). As a sensitivity check we performed two additional analyses: a subset time-interaction analysis restricted to the three main timepoints, and a paired t-test analysis on subjects who transitioned from CN to MCI or MCI to AD across any time interval for each metabolite. A metabolite was considered to significantly change longitudinally with disease if it showed: (i) significance in both the full and subset time-interaction analysis; (ii) significance in the full time-interaction analysis ($p < 4.1 \times 10^{-4}$; Figure 3) and paired t-test analysis ($p < 0.05$); or (iii) significance in all the three analyses. In case of associations with time-resolved diagnostic status, no additional criteria were assessed.

Using the aforementioned criteria, we identified 19 metabolites (3.75%) that were significantly associated. These included aspartic acid, leucine, betaine, valine, cysteine, glutamate, phenylalanine, serine, xanthine, choline, the LPCs C16:1, C17:0, C18:0, and C18:1, PC ae C32:3, PC ae C40:4, PC ae C40:5, PC ae C42:4, and PC ae C42:5. Among these, valine, LPC C16:1, LPC C17:0, and PC ae C32:3 were supported by both the full time-interaction analysis and paired t-test analysis (**Supplementary Table S15**), while betaine and the remaining four PCs were significant in the full time-interaction analysis associated with the time-resolved diagnostic status. The remaining metabolites were consistently significant in both the full and subset time-interaction analysis with aspartic acid showing all three lines of evidence. From a phenotype perspective, grey matter volume and grey matter thickness (n=7 metabolites each) exhibited the largest number of metabolite associations **(Supplementary Table S10; Supplementary Figure S4).**

3.4. Association patterns observed across the different analyses

To directly compare cross-sectional and longitudinal results, we defined concordant effects as associations with the same effect size direction across single timepoint cross-sectional or multi-timepoint meta-analysis and the time-interaction analysis, and discordant effects as associations with opposite effect size directions. Concordant effects were observed for the branched-chain amino acids valine and leucine, which showed consistently lower levels in individuals with reduced grey matter volume in both the multi-timepoint meta-analysis and the time-interaction analysis. Cysteine also demonstrated a concordant positive association with AD versus CN, detectable both in the 12-month cross-sectional analysis and the time-interaction analysis. Notably, cysteine synthesis (expressed as the ratio of cysteine over the sum of serine and methionine) was the only MetaboINDICATOR showing a significant p-gain in the time-interaction analysis for the AD versus CN comparison (see **Supplementary Tables S16-S18** and **Supplementary Figure S3**; p-gain = 3371.48). In contrast, discordant effects were identified for PC ae C40:4, PC ae C42:4, and PC ae C42:5, which showed a positive association with AD in the multi-timepoint meta-analysis but negative associations in the time-interaction analysis. Similarly, choline, phenylalanine, and aspartic acid were elevated at baseline in individuals with AD but declined more sharply over time in the same individuals, leading to opposite effect directions across the two analyses. Phenylalanine and choline were the only persistent metabolites to exhibit a discordant pattern, starting at higher levels and more steeply decreasing levels in AD (as visualized for aspartic acid in **Figure 4b-d**), while the rest of the metabolites were either latent or episodic in nature.

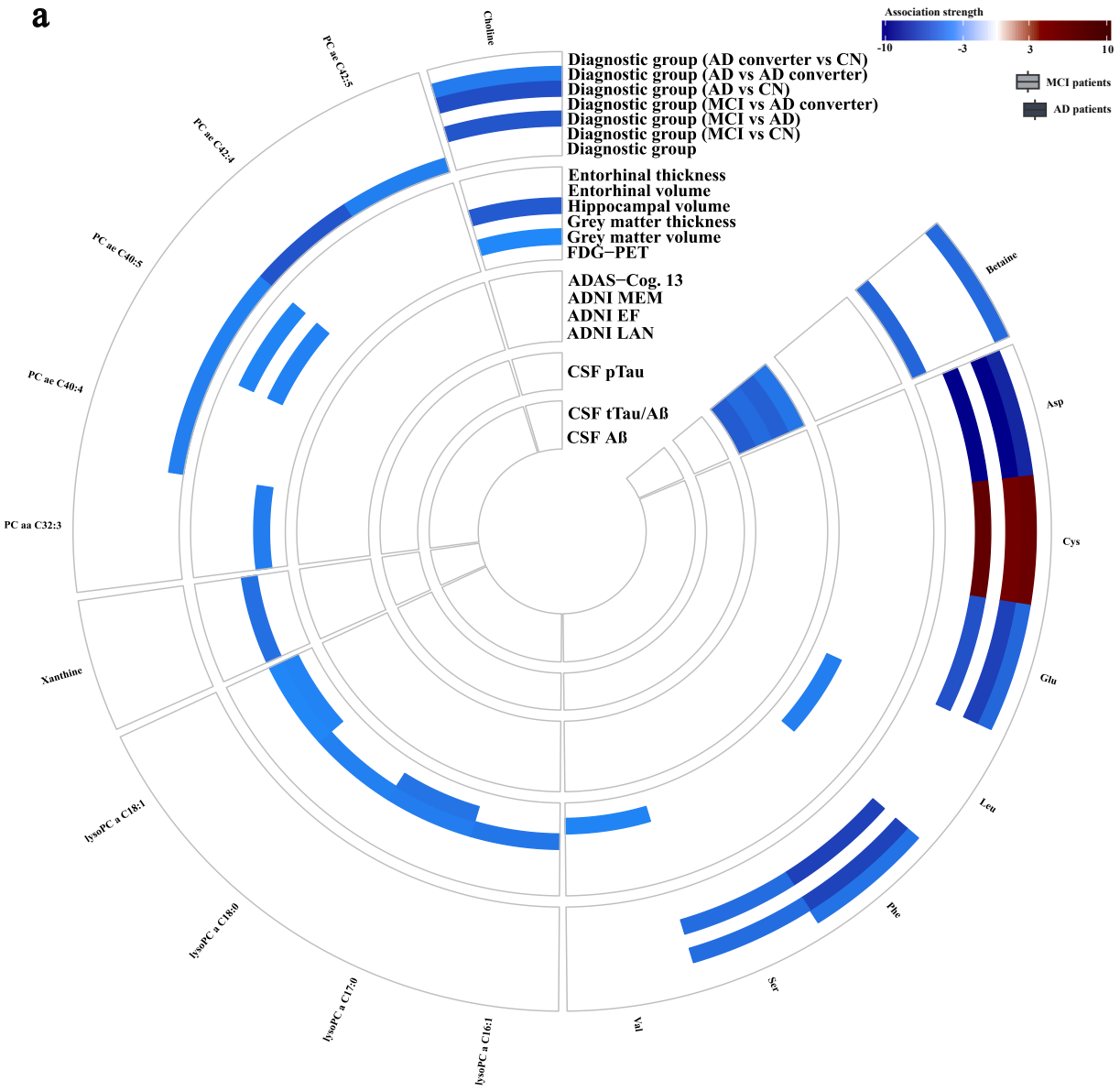
a
Association strength
-10
-3
3
10
MCI patients
AD patients
Diagnostic group (AD converter vs CN)
Diagnostic group (AD vs AD converter)
Diagnostic group (AD vs CN)
Diagnostic group (MCI vs AD converter)
Diagnostic group (MCI vs AD)
Diagnostic group (MCI vs CN)
Diagnostic group
Entorhinal thickness
Entorhinal volume
Hippocampal volume
Grey matter thickness
Grey matter volume
FDG−PET
ADAS−Cog. 13
ADNI MEM
ADNI EF
ADNI LAN
CSF pTau
CSF tTau/Aß
CSF Aß
Choline
PC ae C42:5
PC ae C42:4
PC ae C40:5
PC ae C40:4
PC aa C32:3
Xanthine
lysoPC a C18:1
lysoPC a C18:0
lysoPC a C17:0
lysoPC a C16:1
Val
Ser
Phe
Leu
Glu
Cys
Asp
Betaine

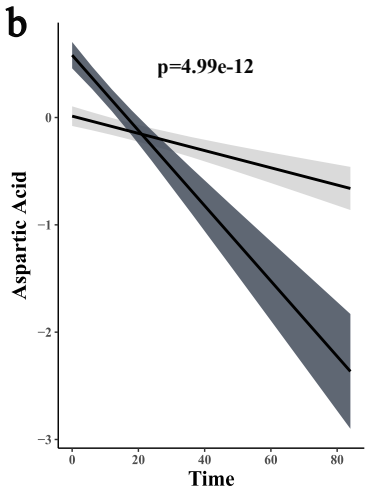
b
p=4.99e-12
Aspartic Acid
Time

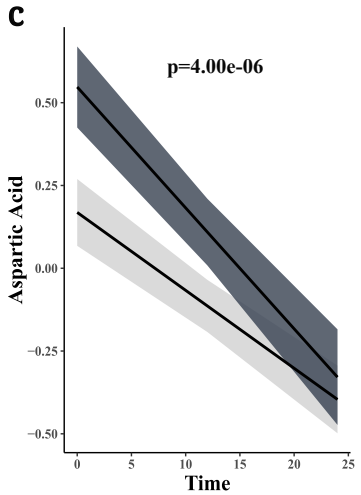
c
p=4.00e-06
Aspartic Acid
Time

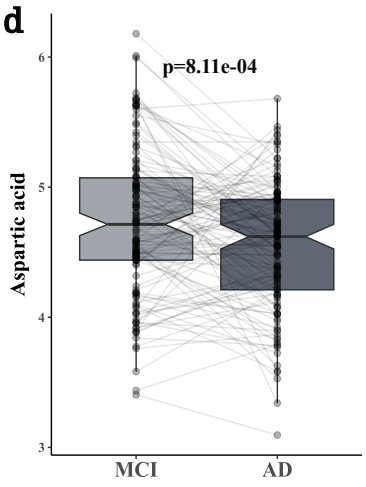
d
p=8.11e-04
Aspartic acid
MCI
AD

Figure 4: Significant associations in time-interaction analysis. (a) Heatmap showing all the significant associations found in time-interaction analysis. Each individual track represents a particular phenotype, red indicates positive associations, i.e. the metabolite levels increase with less desirable phenotypic levels over time, and blue represents negative associations, i.e. metabolite levels tend to decrease with respect to disease over time. Association strength is visualized by $-\log_{10}(p)\cdot\text{sign}(\beta)$ where p is the p-value for the interaction between disease phenotype and time and β is the effect estimate. All effect directions across phenotypes were aligned so that higher beta estimates consistently reflect a worse disease outcome. Metabolites are grouped by the biochemical classes provided by the platform vendor. **(b & c)** Effect plots of the significant association of aspartic acid visualizing its temporal trajectory in MCI and AD in both the full dataset **(b)** and the dataset subset limited to the three main time points **(c)**. The x-axis represents time in months, and the y-axis shows the model-predicted levels of aspartic acid. **(d)** Boxplot illustrating the results of the paired t-test comparing aspartic acid levels for each subject that converted from MCI to AD over a 6-month interval. The x-axis denotes the diagnostic groups, and the y-axis represents levels of aspartic acid. Ribbons around linear fits represent ±1 standard error around the estimate. Box plots display the median (central line), interquartile range (box bounds), whiskers extending to the smallest and largest values within 1.5 times the interquartile range from the quartiles, and notches indicating the 95% confidence interval for the median. All tests were two-sided and raw *p* values were reported. Source data are provided as a Source Data file. *MCI – participants with mild cognitive impairment; AD – participants with clinical Alzheimer's disease.*

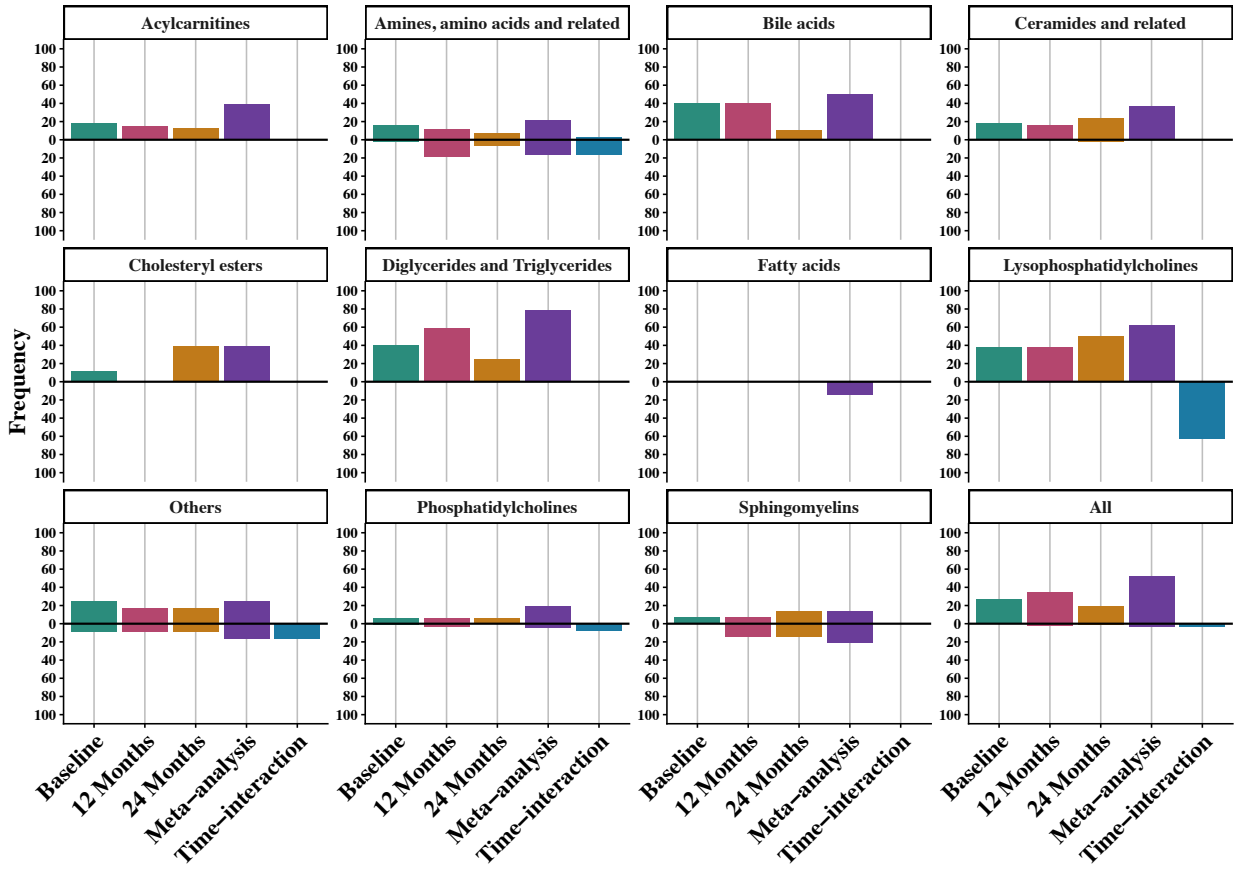

Figure 5: Miami plots representing the frequency (in %) of metabolites significantly associated with any disease phenotype across the different analyses grouped by biochemical classes. Frequencies of positive associations with disease are displayed above zero, negative associations are shown below

zero, but frequency values are expressed as positive percentages in both directions. “Others” here combines metabolite classes with only few representatives, such as hexose, indoles and derivatives, choline, and cortisol (**Supplementary Table S2**). Source data are provided as a Source Data file.

To assess whether these trends extended to the metabolite-class level, we quantified the proportion of metabolites in each class that were significantly associated with any AD phenotype **(Figure 5)**. This revealed several patterns: Acylcarnitines, ceramides (including hexosyl-ceramides), bile acids, TGs, and DGs showed frequent associations in both single timepoint cross-sectional analyses and in the multi-timepoint meta-analysis, but none in the time-interaction analysis. CEs had few associations at baseline but a greater number at later follow-up (24 months), but without further significant evidence from the time-interaction analysis. PCs and LPCs were elevated in disease at baseline but declined over time in relation to less favorable phenotypes. Fatty acids were reduced in individuals with less favorable phenotypes, with no significant associations detected in the time-interaction analysis. Finally, SMs, amino acids and biogenic amines, and several other metabolites (such as hexose, indoles and derivatives, choline, and cortisol; **Supplementary Table S2**) displayed variable or metabolite-specific associations, without a consistent class-level trend besides most metabolites within these classes (except for cysteine) declining over time along the disease trajectory in the time-interaction analysis.

4. Discussion

In this study, we evaluated the temporal patterns of associations between serum metabolites and AD, distinguishing between persistent, latent and episodic associations (ordered by strongest to weakest statistical support) on the one hand and metabolites showing evolving changes in relation to AD on the other hand. Overall, we identified 311 metabolites significantly associated with at least one AD-related phenotype across the different analyses. Most associations were detected in the multi-timepoint meta-analysis (n=281) followed by cross-sectional associations at single timepoints (n=243), while 19 were identified through time-interaction analysis, wherein longitudinal shifts in level differences in relation to disease outcomes were assessed. All study results are also available through an interactive web portal at https://metabolomics.helmholtz-munich.de/mxtra_ad/.

We assume that the multi-timepoint meta-analysis yielding a larger number of significant associations than the analyses of single timepoints to be mostly due to increased statistical power in pooled data. However, this, in conjunction with the comparably small number of metabolites showing evolving changes, further suggests that most metabolic alterations in AD do not change substantially anymore once they manifest, albeit effect sizes may vary slightly over time: More than 40% of the reported metabolites were classified as persistent, with replication at both at least one other timepoint and the multi-timepoint meta-analysis. In contrast, less than 10% of metabolites showed episodic associations, without replication across other timepoints or the multi-timepoint meta-analysis. The remaining metabolites classified as latent all showed consistent trends over time as evidenced by significant associations in the multi-timepoint meta-analysis, and only around 40% of them did not show a significant cross-sectional association at one of the three main timepoints.

16 out of 19 metabolites showing significant evolving changes in relation to AD in the time-interaction analysis were also observed as significant either cross-sectionally or in the multi-timepoint meta-analysis. Out of those, 11 were classified as latent or episodic, while phenylalanine, choline, LPC C16:1 and C18:0, as well as PC aa C32:3 were observed to show persistently higher levels in phenotypically more affected individuals but a significant decrease in levels over time in the time-interaction analysis. Indeed, except for cysteine, we observed negative associations, i.e., a steeper decrease of metabolite levels in phenotypically more affected individuals, for all metabolites that showed evolving level differences in relation to disease phenotypes. This is of particular interest for metabolites like PC ae 42:4, which this and other work discovered to be elevated in blood of AD patients [38]. As we show that the levels of this metabolite decline faster in AD over time, this may result in discrepant findings when looking at individuals with late-stage AD.

Comparing our results to previous studies, we found that a large fraction of the metabolites identified here across biochemical classes have been reported to be linked to AD before [4, 39, 40]. For example, our findings on sphingomyelins are consistent with prior work implicating these lipids in AD pathogenesis, alongside elevated ceramides and cholesteryl esters associated with worse outcomes [41-44]. Similarly, elevated secondary conjugated bile acids have been previously reported for AD in plasma, serum and brain samples, which is in alignment with our findings [5, 45, 46]. LPC C16:1 and LPC C18:1 were reported to be elevated in MCI and linked to memory decline, showing a longitudinal pattern of early increase followed by later depletion [40, 47]. Elevated cortisol levels were reported to reflect systemic stress, consistent with brain, CSF, and plasma studies in AD and linked to brain atrophy and pathological protein accumulation [48, 49]. Creatinine, a product of muscle breakdown and nitrogen clearance and an early (8-15 years prior to symptoms) marker of frailty and dementia risk [50-52], was robustly associated with AD in our analysis. Hippuric acid, a diet- and gut microbiota-derived metabolite associated with cognitive and physical resilience [53], showed a negative association with AD, in line with previous animal studies [54, 55]. Previous studies have further identified PCs to be associated with AD, although some of our findings seem to be novel [38, 44, 56, 57]. Finally, we showed that almost three quarters of the lipid associations reported here were replicated in an independently generated lipidomics dataset, with replication rates dropping from close to 90% for persistent metabolite associations down to 20% for episodic metabolite associations as expected.

Together, the presented work replicates and expands on previously reported metabolite associations with AD. In the following discussion, we highlight a few metabolic domains and molecular pathways that seem to be particularly implicated in the disease through our current and previous findings.

4.1 Bioenergetic dysfunction as a chronic feature of AD

Our study expands upon existing evidence of altered energy metabolism in AD [58]. We found individuals with AD to exhibit elevated TGs, medium- and long-chain acylcarnitines, and reduced free fatty acids in the multi-timepoint meta-analysis, potentially indicating a compensatory but dysfunctional shift toward lipid-based energy production [58, 59]. This pattern is consistent with

inefficiencies in mitochondrial β-oxidation or disruption of the carnitine shuttle system [60], underscoring the broader hypothesis of mitochondrial bioenergetic failures in AD, where impaired glucose uptake is thought to necessitate a shift to alternative energy sources [61]. Importantly, many of these lipid alterations, particularly elevated levels of TGs, DGs, and acylcarnitines, were classified as persistent, i.e. consistently and longitudinally associated with AD phenotypes. This suggests that bioenergetic dysfunction represents a chronic feature of AD pathophysiology in both brain and the periphery. Moreover, mitochondrial dysfunction, along with the observed increased levels of homocysteine, can promote breakdown of muscle tissue, which could explain the sustained higher levels of creatinine and alanine we found.

We further observed lower levels of branched-chain amino acids (BCAAs) in AD, with valine and leucine levels correlating with reduced grey matter volume in the multi-timepoint meta-analysis and significantly decreasing levels over time as revealed by the time-interaction analysis. This expands on earlier findings [62, 63] and indicates a progressive decline in BCAA levels, potentially reflecting their increased utilization as alternative energy substrates in the tricarboxylic acid (TCA) cycle. While BCAA supplementation promotes mitochondrial biogenesis and ATP production in malnourished elderly individuals [64-66], their depletion in AD may compromise neuronal energy supply and structural integrity over time. Moreover, BCAA alterations have been linked to insulin resistance and metabolic syndromes such as type 2 diabetes and obesity, which are recognized AD risk factors [67, 68]. Through modulation of the TORC1 pathway, which governs autophagy and cellular aging, chronic BCAA depletion may impair protein turnover, enhance oxidative vulnerability, and contribute to neurodegenerative cascades [69-71]. Finally, BCAAs serve as precursors for neurotransmitters such as glutamate and GABA, which suggests that their depletion may further compromise neurotransmission, linking bioenergetic deficits to synaptic dysfunction [72].

4.2 Impairment of neurotransmission systems worsens with AD progression

Impaired neurotransmission, particularly impaired acetylcholine synthesis and dysbalanced glutamatergic and GABAergic neurotransmission, is a core feature of AD pathology [73, 74]. In line with that, we found that levels of choline (a precursor of the neurotransmitter acetylcholine) were significantly higher in AD cases compared to controls but steeply declining over time with progressing disease. Secondary evidence comes from negative associations of PCs and LPCs in the time-interaction analysis, as they are downstream products of the CDP-choline pathway [75]. This steeper decline observed in AD could point to increased compensatory choline transport into the brain, which in rodents was shown to be dependent on choline demand in brain [76].

Second, we observed GABA to be negatively associated with executive function and grey matter volume in the multi-timepoint meta-analysis, respectively, and a significant negative association of glutamate with diagnostic status in the time-interaction analysis. As mentioned, this reduced glutamate and GABA availability may link back to bioenergetics and could result from BCAA depletion and impaired TCA cycle activity limiting α-ketoglutarate production – one precursor for both glutamate and GABA synthesis [77, 78]. Previous longitudinal studies have also described a dynamic trajectory of glutamate metabolism, where elevated peripheral glutamate levels predict

dementia risk up to 15 years before diagnosis [79], while decreasing levels closer to dementia diagnosis associate with accelerated cognitive decline and inverse brain-serum glutamate correlations [80-84]. This inverse brain-serum correlation could be due to the efflux of glutamate from brain to blood being significantly reduced in more advanced disease stages. Of note, reduced glutamate levels in our data do not appear to stem from increased conversion to glutamine (glutaminase activity in the metaboINDICATOR analysis was not significantly linked to AD). However, compensatory ammonia detoxification may still be implicated in light of the elevated citrulline levels we observed in individuals with worse AD outcomes as well as previously reported findings [85-87].

Third, we identified longitudinal declines in phenylalanine, aspartic acid and serine levels in individuals with AD. These metabolites showed discordant effects, starting with higher but steeply decreasing levels in AD over time, similar to what we observed for choline. Interestingly, in our previous study using metabolomics data from brain tissue, we observed elevated levels of e.g. serine and phenylalanine in AD [7], which could again indicate increased uptake. Changes to the levels of phenylalanine, a precursor for tyrosine and catecholamines (dopamine, norepinephrine), could contribute to dopaminergic and noradrenergic deficits in AD, which is consistent with prior studies in plasma and brain tissue [15, 83, 88-90]. Similarly, altered levels of serine and aspartic acid may impair neurotransmitter function given their role as NMDA receptor agonists [15, 91].

Overall, the metabolic alterations we observed across neurotransmitter pathways point to attempted compensation at earlier disease stages, which breaks apart at some point in the disease trajectory, likely contributing to accelerated decline in later-stage disease.

4.3 Oxidative stress response and antioxidant failure

In addition to its role as neurotransmitter, GABA – as well as AABA – is known to have antioxidant function [92] in response to oxidative stress, which is another key driver of neurodegeneration in AD. We found lower levels of both GABA and AABA to be associated with worse cognitive function and less favorable biomarker profiles, replicating previous work [93].

Interestingly, several other metabolites highlighted here are not only involved in oxidative stress and inflammation but also point to a role for dietary habits and gut microbiome composition. For instance, we found lower levels of tryptophan betaine (lenticin), an anti-inflammatory dietary marker of plant-rich dietary interventions such as Dietary Approaches to Stop Hypertension (DASH) and Mediterranean-DASH Intervention for Neurodegenerative Delay (MIND), to be consistently associated with worse cognitive outcomes across models [94, 95]. We further observed several microbially-derived tryptophan derivatives to be linked to oxidative stress and inflammation in AD. One of those was indoxyl sulfate, a pro-inflammatory tryptophan-derived microbial co-metabolite that is considered a neurotoxin through its activation of acetylcholine receptors. We identified higher levels of indoxyl sulfate to be persistently positively associated with AD, suggesting continuous pro-inflammatory effects, a finding that replicates previous plasma- and brain-based studies [48, 96, 97]. In contrast, lower levels of 3-indolepropionic acid (3-IPA), another microbial tryptophan metabolite known for its anti-inflammatory, antioxidant, and neuroprotective properties [98-100], were associated with poorer cognitive performance, supporting

the notion that shifts in diet- and gut-derived metabolites can influence cognitive trajectories [48, 101]. Prior studies have shown that 3-IPA production can be enhanced by low-fat diets, underscoring the potential of dietary interventions to influence disease risk via gut-brain axis pathways [102].

Conversely, markers of oxidative damage were positively associated with AD phenotypes. For instance, we observed increased levels of SDMA, a marker for oxidative stress, to be persistently associated with AD [103]. We also observed significantly elevated levels of homocysteine. Hyperhomocysteinemia is not only an established risk marker for dementia development but also a blood biomarker for (subclinical) deficiencies of B vitamins, which are involved in oxidative stress response and have been linked to AD as well [16, 79, 104-106].

Finally, we found evidence for potential metabolic adaptation, manifesting in elevated levels of cysteine and glycine in AD. Both metabolites are building blocks of glutathione, one of the central antioxidants, which has been previously linked to AD including in brain [7]. Cysteine further showed increasing levels during disease progression and cysteine synthesis (here approximated by the ratio of cysteine and the sum of serine and methionine) was the only MetaboINDICATOR in our study showing a significant change over time. This could indicate an attempt of the system to compensate for oxidative stress/vitamin B deficiency by an increased conversion of homocysteine (through conjugation with serine, which we found significantly decreasing with disease over time) to cysteine as response [85-87, 107-109].

However, cysteine is also a precursor for coenzyme A, implicating it additionally in mitochondrial oxidative bioenergetics, including the TCA cycle and β-oxidation [110, 111]. Oxidative stress is exacerbated by and contributes to mitochondrial dysfunction. Furthermore, as mentioned in the context of neurotransmission, we found the levels of the third building block of glutathione, glutamate, to be significantly decreasing with disease progression. Therefore, despite the large body of insights added by our study, the interconnectedness of metabolism makes it complex to fully disentangle cause and consequence of the reported metabolic alterations.

4.4 Limitations and potential for future work

There are several limitations to our study. First, the ADNI cohort predominantly includes older adults of Caucasian descent, which may limit generalizability to younger or more diverse populations, as both age, racioethnic background, and genetics influence metabolic profiles in AD. Second, averaging across participants may obscure inter-individual variability in disease progression. Some individuals decline more rapidly than others, and this heterogeneity could mask relevant metabolic dynamics. Stratifying participants by progression rates in future research can address this limitation. Moreover, due to ADNI's strict exclusion criteria, frequent comorbidities such as cardiovascular conditions could not be analyzed in detail and interpreted adequately. Third, CSF measures were predominantly available only at baseline, restricting our ability to assess longitudinal associations between metabolite levels and levels of AD biomarkers in CSF. Incorporating amyloid- and tau-PET measurements, as well as the evolving blood biomarkers, will be key for assessing temporal changes between central biomarkers and peripheral metabolism. Fourth, although consistent trends were observed at the lipid class level,

interpretation at the species level remains limited due to unresolved acyl chain composition and desaturation sites. This lack of resolution hinders precise mapping to specific metabolic pathways and biological functions. Additionally, the metabolomics platform used in this study is primarily focused on lipids. Future studies using broader, untargeted platforms could provide a more comprehensive characterization of the biochemical alterations associated with AD. Fifth, longitudinal studies like ours need to be integrated with data from paired blood- and brain tissue-based metabolomics to enable the study of cross-compartmental metabolic dynamics. Together with genetic analyses, this will be essential to ultimately identify causal factors. Lastly, dietary intake and gut microbiome composition, known to strongly influence circulating metabolites [112, 113], were not accounted for in the current study but could be very informative, especially for pathways such as bile acid metabolism and tryptophan degradation highlighted here.

4.5 Conclusion

In summary, this study provides a systematic evaluation of metabolic alterations in Alzheimer's disease, distinguishing between persistent, latent, and episodic associations, as well as those that continue to change over time. Our findings highlight widespread and interconnected alterations to lipid, amino acid, oxidative stress, energy, and neurotransmitter metabolism. Our results emphasize the robustness and somewhat limited dynamic nature of metabolic changes in AD in an elderly study cohort and the importance of temporal context when interpreting metabolomics data. The large amount of chronic metabolic differences in AD points at windows for therapeutic interventions targeting the implicated pathways. Future studies integrating dietary and gut microbiome data, as well as more diverse ethnic backgrounds will be essential to further understand these trajectories, their mechanistic underpinnings, and to identify potentially modifiable factors.

Data availability

The results published here are in whole or in part based on data obtained from the AD Knowledge Portal (https://adknowledgeportal.org). The AD Knowledge Portal is a platform for accessing data, analyses, and tools generated by the Accelerating Medicines Partnership (AMP-AD) Target Discovery Program and other National Institute on Aging (NIA)-supported programs to enable open-science practices and accelerate translational learning. The data, analyses, and tools are shared early in the research cycle without a publication embargo on secondary use. Data are available for general research use according to the following requirements for data access and data attribution (https://adknowledgeportal.org/DataAccess/Instructions). ADNI longitudinal metabolomics data can be accessed under https://doi.org/10.7303/9618123. All other data, including the full complement of clinical and demographic data for the ADNI cohorts are hosted on the LONI data sharing platform and can be requested at https://adni.loni.usc.edu/data-samples/adni-data/#AccessData. All summary statistics as well as additional information and visualizations are available online at https://metabolomics.helmholtz-munich.de/mxtra_ad/. Source data are provided with this paper.

Code availability

All R code required to conduct the analyses reported here is available at https://github.com/compneurobio/mxtra-ad.

Acknowledgements

This work was supported by the National Institutes of Health/the National Institute of Aging through grants R01AG069901, U01AG088562, and R01AG081322. Metabolomics data is provided by the Alzheimer's Disease Metabolomics Consortium (ADMC) and funded wholly or in part by the following grants and supplements thereto: NIA U19AG063744, R01AG046171, RF1AG057452, R01AG059093, RF1AG058942, U01AG061359, awarded to Dr. Kaddurah-Daouk at Duke University in partnership with a large number of academic institutions. As such, the investigators within the ADMC, not listed specifically in this publication's author's list, provided data along with its pre-processing and prepared it for analysis, but did not participate in analysis or writing of this manuscript. A complete listing of ADMC investigators can be found at: https://sites.duke.edu/adnimetab/team/. The Biocrates Q500 data was generated at Duke University. Data collection and sharing for this project was funded by the Alzheimer's Disease Neuroimaging Initiative (ADNI) (National Institutes of Health Grant U01 AG024904) and DOD ADNI (Department of Defense award number W81XWH-12-2-0012). ADNI is funded by the National Institute on Aging, the National Institute of Biomedical Imaging and Bioengineering, and through generous contributions from the following: AbbVie, Alzheimer's Association; Alzheimer's Drug Discovery Foundation; Araclon Biotech; BioClinica, Inc.; Biogen; Bristol-Myers Squibb Company; CereSpir, Inc.; Cogstate; Eisai Inc.; Elan Pharmaceuticals, Inc.; Eli Lilly and Company; EuroImmun; F. Hoffmann-La Roche Ltd and its affiliated company Genentech, Inc.; Fujirebio; GE Healthcare; IXICO Ltd.; Janssen Alzheimer Immunotherapy Research & Development, LLC.; Johnson & Johnson Pharmaceutical Research & Development LLC.; Lumosity; Lundbeck; Merck

& Co., Inc.; Meso Scale Diagnostics, LLC.; NeuroRx Research; Neurotrack Technologies; Novartis Pharmaceuticals Corporation; Pfizer Inc.; Piramal Imaging; Servier; Takeda Pharmaceutical Company; and Transition Therapeutics. The Canadian Institutes of Health Research is providing funds to support ADNI clinical sites in Canada. Private sector contributions are facilitated by the Foundation for the National Institutes of Health (www.fnih.org). The grantee organization is the Northern California Institute for Research and Education, and the study is coordinated by the Alzheimer's Therapeutic Research Institute at the University of Southern California. ADNI data are disseminated by the Laboratory for Neuro Imaging at the University of Southern California. KH is supported by a National Health and Medical Research Council (NHMRC) investigator grant (#1197190).

Author contributions

Conceptualization: PJM, GK, RK-D, MA; **Data curation:** BM, PW, SLR, CB, NK, KK, AK-P, JWT, TB, KN, AJS, MA; **Collection of clinical data:** PMD; **Formal analysis:** BM, PW, MA; **Funding acquisition:** GK, RK-D, MA; **Investigation:** BM, PW, JJB, NK, KK, JWT, GK, MA; **Methodology:** BM, PW, TW, KH, JWT, MA; **Project administration:** CB, AK-P, GK, RK-D, MA; **Software:** BM, PW, MA; **Supervision:** PJM, GK, RK-D, MA; **Visualization:** BM, PW, JJB, GK, MA; **Writing – original draft:** BM, PW, JJB, MA; **Writing – review & editing:** All authors

Competing interests

AJS is a member of the Scientific Advisory Board of Bayer Oncology and of the Dementia Advisory Board of Siemens Medical Solutions USA, Inc.; AJS received in-kind support from Avid Radiopharmaceuticals, a subsidiary of Eli Lilly (PET tracer precursor); AJS received Editorial Office Support as Editor-in-Chief from Springer-Nature Publishing (Brain Imaging and Behavior). PMD has received research grants or gifts (through Duke University) from NIH, ADNI, Columbia University, Steve Aoki Foundation, lululemon, Gates Ventures, DOD, Fordham University, and Cure Alzheimer Fund; PMD has received advisory fees from Alzheon, Lumos Labs, UMethod, Transposon Therapeutics, Neurology Live and Prospira; PMD owns shares or options in UMethod, Evidation Health, Transposon, Marvel Biome and Alzheon; PMD serves on the board of Apollo and is a co-inventor (through Duke University) on patents relating to dementia biomarkers, metabolomics, and therapies. RK-D holds equity in Metabolon Inc., which had no role in this work. MA, RK-D, and GK are co-inventors (through Duke University/Helmholtz Zentrum München) on patents on applications of metabolomics in diseases of the central nervous system; MA, RK-D, and GK hold equity in Chymia LLC, which had no role in this work.

References

1. Querfurth HW, LaFerla FM. Alzheimer's disease. N Engl J Med. 2010;362(4):329–44. doi: 10.1056/NEJMra0909142. PubMed PMID: 20107219.
2. Trushina E, Dutta T, Persson XM, Mielke MM, Petersen RC. Identification of altered metabolic pathways in plasma and CSF in mild cognitive impairment and Alzheimer's disease using metabolomics. PLoS One. 2013;8(5):e63644. Epub 20130520. doi: 10.1371/journal.pone.0063644. PubMed PMID: 23700429; PMCID: PMC3658985.
3. Han X, Rozen S, Boyle SH, Hellegers C, Cheng H, Burke JR, Welsh-Bohmer KA, Doraiswamy PM, Kaddurah-Daouk R. Metabolomics in early Alzheimer's disease: identification of altered plasma sphingolipidome using shotgun lipidomics. PLoS One. 2011;6(7):e21643. Epub 20110711. doi: 10.1371/journal.pone.0021643. PubMed PMID: 21779331; PMCID: PMC3136924.
4. Toledo JB, Arnold M, Kastenmuller G, Chang R, Baillie RA, Han X, Thambisetty M, Tenenbaum JD, Suhre K, Thompson JW, John-Williams LS, MahmoudianDehkordi S, Rotroff DM, Jack JR, Motsinger-Reif A, Risacher SL, Blach C, Lucas JE, Massaro T, Louie G, Zhu H, Dallmann G, Klavins K, Koal T, Kim S, Nho K, Shen L, Casanova R, Varma S, Legido-Quigley C, Moseley MA, Zhu K, Henrion MYR, van der Lee SJ, Harms AC, Demirkan A, Hankemeier T, van Duijn CM, Trojanowski JQ, Shaw LM, Saykin AJ, Weiner MW, Doraiswamy PM, Kaddurah-Daouk R, Alzheimer's Disease Neuroimaging I, the Alzheimer Disease Metabolomics C. Metabolic network failures in Alzheimer's disease: A biochemical road map. Alzheimers Dement. 2017;13(9):965–84. Epub 20170322. doi: 10.1016/j.jalz.2017.01.020. PubMed PMID: 28341160; PMCID: PMC5866045.
5. MahmoudianDehkordi S, Arnold M, Nho K, Ahmad S, Jia W, Xie G, Louie G, Kueider-Paisley A, Moseley MA, Thompson JW, St John Williams L, Tenenbaum JD, Blach C, Baillie R, Han X, Bhattacharyya S, Toledo JB, Schafferer S, Klein S, Koal T, Risacher SL, Kling MA, Motsinger-Reif A, Rotroff DM, Jack J, Hankemeier T, Bennett DA, De Jager PL, Trojanowski JQ, Shaw LM, Weiner MW, Doraiswamy PM, van Duijn CM, Saykin AJ, Kastenmuller G, Kaddurah-Daouk R, Alzheimer's Disease Neuroimaging I, the Alzheimer Disease Metabolomics C. Altered bile acid profile associates with cognitive impairment in Alzheimer's disease-An emerging role for gut microbiome. Alzheimers Dement. 2019;15(1):76–92. Epub 20181015. doi: 10.1016/j.jalz.2018.07.217. PubMed PMID: 30337151; PMCID: PMC6487485.
6. Ambeskovic M, Hopkins G, Hoover T, Joseph JT, Montina T, Metz GAS. Metabolomic Signatures of Alzheimer's Disease Indicate Brain Region-Specific Neurodegenerative Progression. Int J Mol Sci. 2023;24(19):14769–. Epub 20230930. doi: 10.3390/ijms241914769. PubMed PMID: 37834217; PMCID: PMC10573054.
7. Batra R, Arnold M, Worheide MA, Allen M, Wang X, Blach C, Levey AI, Seyfried NT, Ertekin-Taner N, Bennett DA, Kastenmuller G, Kaddurah-Daouk RF, Krumsiek J, Alzheimer's Disease Metabolomics C. The landscape of metabolic brain alterations in Alzheimer's disease. Alzheimers Dement. 2023;19(3):980–98. Epub 20220713. doi: 10.1002/alz.12714. PubMed PMID: 35829654; PMCID: PMC9837312.
8. Tian Q, Yao S, Marron MM, Greig EE, Shore S, Ferrucci L, Shah R, Murthy VL, Newman AB. Shared plasma metabolomic profiles of cognitive and mobility decline predict future dementia. Geroscience. 2024;46(5):4883–94. Epub 20240603. doi: 10.1007/s11357-024-01228-7. PubMed PMID: 38829458; PMCID: PMC11336156.
9. Akyuz E, Arulsamy A, Aslan FS, Sarisozen B, Guney B, Hekimoglu A, Yilmaz BN, Retinasamy T, Shaikh MF. An Expanded Narrative Review of Neurotransmitters on Alzheimer's Disease: The Role of Therapeutic Interventions on Neurotransmission. Mol Neurobiol. 2025;62(2):1631–74. Epub 20240716. doi: 10.1007/s12035-024-04333-y. PubMed PMID: 39012443; PMCID: PMC11772559.

10. Pillet LE, Taccola C, Cotoni J, Thiriez H, André K, Verpillot R. Correlation between cognition and plasma noradrenaline level in Alzheimer's disease: a potential new blood marker of disease evolution. Translational Psychiatry. 2020;10(1):1–10. doi: 10.1038/S41398-020-0841-7;TECHMETA.
11. Knornschild F, Zhang EJ, Ghosh Biswas R, Kobus M, Chen J, Zhou JX, Rao A, Sun J, Wang X, Li W, Muti IH, Habbel P, Nowak J, Xie Z, Zhang Y, Cheng LL. Correlations of blood and brain NMR metabolomics with Alzheimer's disease mouse models. Transl Psychiatry. 2025;15(1):87. Epub 20250318. doi: 10.1038/s41398-025-03293-8. PubMed PMID: 40102403; PMCID: PMC11920067.
12. Ahmad S, Yang W, Orellana A, Frolich L, de Rojas I, Cano A, Boada M, Hernandez I, Hausner L, Harms AC, Bakker MHM, Cabrera-Socorro A, Amin N, Ramirez A, Ruiz A, Van Duijn CM, Hankemeier T. Association of oxidative stress and inflammatory metabolites with Alzheimer's disease cerebrospinal fluid biomarkers in mild cognitive impairment. Alzheimers Res Ther. 2024;16(1):171. Epub 20240730. doi: 10.1186/s13195-024-01542-4. PubMed PMID: 39080778; PMCID: PMC11287840.
13. Dronse J, Ohndorf A, Richter N, Bischof GN, Fassbender R, Behfar Q, Gramespacher H, Dillen K, Jacobs HIL, Kukolja J, Fink GR, Onur OA. Serum cortisol is negatively related to hippocampal volume, brain structure, and memory performance in healthy aging and Alzheimer's disease. Front Aging Neurosci. 2023;15:1154112. Epub 20230512. doi: 10.3389/fnagi.2023.1154112. PubMed PMID: 37251803; PMCID: PMC10213232.
14. Mosconi L, Williams S, Carlton C, Zarate C, Boneu C, Fauci F, Ajila T, Nerattini M, Jett S, Andy C, Battista M, Pahlajani S, Osborne J, Brinton RD, Dyke JP. Sex-specific associations of serum cortisol with brain biomarkers of Alzheimer's risk. Sci Rep. 2024;14(1):5519. Epub 20240306. doi: 10.1038/s41598-024-56071-9. PubMed PMID: 38448497; PMCID: PMC10918173.
15. Xu J, Begley P, Church SJ, Patassini S, Hollywood KA, Jullig M, Curtis MA, Waldvogel HJ, Faull RL, Unwin RD, Cooper GJ. Graded perturbations of metabolism in multiple regions of human brain in Alzheimer's disease: Snapshot of a pervasive metabolic disorder. Biochim Biophys Acta. 2016;1862(6):1084–92. Epub 20160305. doi: 10.1016/j.bbadis.2016.03.001. PubMed PMID: 26957286; PMCID: PMC4856736.
16. de Leeuw FA, Peeters CFW, Kester MI, Harms AC, Struys EA, Hankemeier T, van Vlijmen HWT, van der Lee SJ, van Duijn CM, Scheltens P, Demirkan A, van de Wiel MA, van der Flier WM, Teunissen CE. Blood-based metabolic signatures in Alzheimer's disease. Alzheimers Dement (Amst). 2017;8(1):196–207. Epub 20170906. doi: 10.1016/j.dadm.2017.07.006. PubMed PMID: 28951883; PMCID: PMC5607205.
17. Kurbatova N, Garg M, Whiley L, Chekmeneva E, Jimenez B, Gomez-Romero M, Pearce J, Kimhofer T, D'Hondt E, Soininen H, Kloszewska I, Mecocci P, Tsolaki M, Vellas B, Aarsland D, Nevado-Holgado A, Liu B, Snowden S, Proitsi P, Ashton NJ, Hye A, Legido-Quigley C, Lewis MR, Nicholson JK, Holmes E, Brazma A, Lovestone S. Urinary metabolic phenotyping for Alzheimer's disease. Sci Rep. 2020;10(1):21745. Epub 20201210. doi: 10.1038/s41598-020-78031-9. PubMed PMID: 33303834; PMCID: PMC7730184.
18. Mielke MM, Haughey NJ, Bandaru VV, Schech S, Carrick R, Carlson MC, Mori S, Miller MI, Ceritoglu C, Brown T, Albert M, Lyketsos CG. Plasma ceramides are altered in mild cognitive impairment and predict cognitive decline and hippocampal volume loss. Alzheimers Dement. 2010;6(5):378–85. doi: 10.1016/j.jalz.2010.03.014. PubMed PMID: 20813340; PMCID: PMC2933928.
19. Huang YL, Chang WJ, Lin CH, Zhang S, Nishita Y, Otsuka R, Lee WJ, Liang CK, Chou MY, Peng LN, Arai H, Ferrucci L, Chen LK. Data from multi-national aging cohorts show dysregulated metabolic pathways in people with physio-cognitive decline. Commun Med (Lond). 2025;5(1):351. Epub 20250814. doi: 10.1038/s43856-025-01073-5. PubMed PMID: 40813794; PMCID: PMC12354693.

20. Lawrence E, Vegvari C, Ower A, Hadjichrysanthou C, De Wolf F, Anderson RM. A Systematic Review of Longitudinal Studies Which Measure Alzheimer's Disease Biomarkers. J Alzheimers Dis. 2017;59(4):1359–79. doi: 10.3233/JAD-170261. PubMed PMID: 28759968; PMCID: PMC5611893.
21. Wang T, Arnold M, Huynh K, Weinisch P, Giles C, Mellett NA, Duong T, Marella B, Nho K, De Livera A, Han X, Blach C, Yu C, McNeil JJ, Lacaze P, Saykin AJ, Kastenmuller G, Meikle PJ, Kaddurah-Daouk R, Alzheimer's Disease Neuroimaging I. Trajectory of plasma lipidome associated with the risk of late-onset Alzheimer's disease: a longitudinal cohort study. EBioMedicine. 2025;118:105826. Epub 20250630. doi: 10.1016/j.ebiom.2025.105826. PubMed PMID: 40592256; PMCID: PMC12269576.
22. Mueller SG, Weiner MW, Thal LJ, Petersen RC, Jack C, Jagust W, Trojanowski JQ, Toga AW, Beckett L. The Alzheimer's disease neuroimaging initiative. Neuroimaging Clin N Am. 2005;15(4):869–77, xi–xii. doi: 10.1016/j.nic.2005.09.008. PubMed PMID: 16443497; PMCID: PMC2376747.
23. Weiner MW, Veitch DP, Aisen PS, Beckett LA, Cairns NJ, Cedarbaum J, Donohue MC, Green RC, Harvey D, Jack CR, Jr., Jagust W, Morris JC, Petersen RC, Saykin AJ, Shaw L, Thompson PM, Toga AW, Trojanowski JQ, Alzheimer's Disease Neuroimaging I. Impact of the Alzheimer's Disease Neuroimaging Initiative, 2004 to 2014. Alzheimers Dement. 2015;11(7):865–84. doi: 10.1016/j.jalz.2015.04.005. PubMed PMID: 26194320; PMCID: PMC4659407.
24. Jack CR, Jr., Bennett DA, Blennow K, Carrillo MC, Feldman HH, Frisoni GB, Hampel H, Jagust WJ, Johnson KA, Knopman DS, Petersen RC, Scheltens P, Sperling RA, Dubois B. A/T/N: An unbiased descriptive classification scheme for Alzheimer disease biomarkers. Neurology. 2016;87(5):539–47. Epub 20160701. doi: 10.1212/WNL.0000000000002923. PubMed PMID: 27371494; PMCID: PMC4970664.
25. Hansson O, Seibyl J, Stomrud E, Zetterberg H, Trojanowski JQ, Bittner T, Lifke V, Corradini V, Eichenlaub U, Batrla R, Buck K, Zink K, Rabe C, Blennow K, Shaw LM, Swedish Bio Fsg, Alzheimer's Disease Neuroimaging I. CSF biomarkers of Alzheimer's disease concord with amyloid-beta PET and predict clinical progression: A study of fully automated immunoassays in BioFINDER and ADNI cohorts. Alzheimers Dement. 2018;14(11):1470–81. Epub 20180301. doi: 10.1016/j.jalz.2018.01.010. PubMed PMID: 29499171; PMCID: PMC6119541.
26. Bittner T, Zetterberg H, Teunissen CE, Ostlund RE, Jr., Militello M, Andreasson U, Hubeek I, Gibson D, Chu DC, Eichenlaub U, Heiss P, Kobold U, Leinenbach A, Madin K, Manuilova E, Rabe C, Blennow K. Technical performance of a novel, fully automated electrochemiluminescence immunoassay for the quantitation of beta-amyloid (1-42) in human cerebrospinal fluid. Alzheimers Dement. 2016;12(5):517–26. Epub 20151110. doi: 10.1016/j.jalz.2015.09.009. PubMed PMID: 26555316.
27. Jack CR, Jr., Bernstein MA, Fox NC, Thompson P, Alexander G, Harvey D, Borowski B, Britson PJ, J LW, Ward C, Dale AM, Felmlee JP, Gunter JL, Hill DL, Killiany R, Schuff N, Fox-Bosetti S, Lin C, Studholme C, DeCarli CS, Krueger G, Ward HA, Metzger GJ, Scott KT, Mallozzi R, Blezek D, Levy J, Debbins JP, Fleisher AS, Albert M, Green R, Bartzokis G, Glover G, Mugler J, Weiner MW. The Alzheimer's Disease Neuroimaging Initiative (ADNI): MRI methods. J Magn Reson Imaging. 2008;27(4):685–91. doi: 10.1002/jmri.21049. PubMed PMID: 18302232; PMCID: PMC2544629.
28. Fischl B, Salat DH, Busa E, Albert M, Dieterich M, Haselgrove C, van der Kouwe A, Killiany R, Kennedy D, Klaveness S, Montillo A, Makris N, Rosen B, Dale AM. Whole brain segmentation: automated labeling of neuroanatomical structures in the human brain. Neuron. 2002;33(3):341–55. doi: 10.1016/s0896-6273(02)00569-x. PubMed PMID: 11832223.

29. Fischl B, Dale AM. Measuring the thickness of the human cerebral cortex from magnetic resonance images. Proc Natl Acad Sci U S A. 2000;97(20):11050–5. doi: 10.1073/pnas.200033797. PubMed PMID: 10984517; PMCID: PMC27146.
30. Landau SM, Harvey D, Madison CM, Koeppe RA, Reiman EM, Foster NL, Weiner MW, Jagust WJ, Alzheimer's Disease Neuroimaging I. Associations between cognitive, functional, and FDG-PET measures of decline in AD and MCI. Neurobiol Aging. 2011;32(7):1207–18. Epub 20090805. doi: 10.1016/j.neurobiolaging.2009.07.002. PubMed PMID: 19660834; PMCID: PMC2891865.
31. Jagust WJ, Bandy D, Chen K, Foster NL, Landau SM, Mathis CA, Price JC, Reiman EM, Skovronsky D, Koeppe RA, Alzheimer's Disease Neuroimaging I. The Alzheimer's Disease Neuroimaging Initiative positron emission tomography core. Alzheimers Dement. 2010;6(3):221–9. doi: 10.1016/j.jalz.2010.03.003. PubMed PMID: 20451870; PMCID: PMC2920531.
32. St John-Williams L, Blach C, Toledo JB, Rotroff DM, Kim S, Klavins K, Baillie R, Han X, Mahmoudiandehkordi S, Jack J, Massaro TJ, Lucas JE, Louie G, Motsinger-Reif AA, Risacher SL, Alzheimer's Disease Neuroimaging I, Alzheimer's Disease Metabolomics C, Saykin AJ, Kastenmuller G, Arnold M, Koal T, Moseley MA, Mangravite LM, Peters MA, Tenenbaum JD, Thompson JW, Kaddurah-Daouk R. Targeted metabolomics and medication classification data from participants in the ADNI1 cohort. Sci Data. 2017;4(1):170140. Epub 20171017. doi: 10.1038/sdata.2017.140. PubMed PMID: 29039849; PMCID: PMC5644370.
33. Breiman L. Random forests. Machine Learning. 2001;45(1):5–32. doi: Doi 10.1023/A:1010933404324. PubMed PMID: WOS:000170489900001.
34. Kursa MB, Jankowski A, Rudnicki WR. Boruta - A System for Feature Selection. Fundamenta Informaticae. 2010;101(4):271–86. doi: 10.3233/Fi-2010-288. PubMed PMID: WOS:000282465600002.
35. Kursa MB, Rudnicki WR. Feature Selection with theBorutaPackage. Journal of Statistical Software. 2010;36(11):1–13. doi: 10.18637/jss.v036.i11.
36. Li J, Ji L. Adjusting multiple testing in multilocus analyses using the eigenvalues of a correlation matrix. Heredity (Edinb). 2005;95(3):221–7. doi: 10.1038/sj.hdy.6800717. PubMed PMID: 16077740.
37. Petersen AK, Krumsiek J, Wagele B, Theis FJ, Wichmann HE, Gieger C, Suhre K. On the hypothesis-free testing of metabolite ratios in genome-wide and metabolome-wide association studies. BMC Bioinformatics. 2012;13(1):120. Epub 20120606. doi: 10.1186/1471-2105-13-120. PubMed PMID: 22672667; PMCID: PMC3537592.
38. Wilkins JM, Trushina E. Application of Metabolomics in Alzheimer's Disease. Front Neurol. 2017;8(JAN):719. Epub 20180112. doi: 10.3389/fneur.2017.00719. PubMed PMID: 29375465; PMCID: PMC5770363.
39. Chen T, Wang L, Xie G, Kristal BS, Zheng X, Sun T, Arnold M, Louie G, Li M, Wu L, Mahmoudiandehkordi S, Sniatynski MJ, Borkowski K, Guo Q, Kuang J, Wang J, Nho K, Ren Z, Kueider-Paisley A, Blach C, Kaddurah-Daouk R, Jia W, Alzheimer's Disease Neuroimaging I, the Alzheimer Disease Metabolomics C. Serum Bile Acids Improve Prediction of Alzheimer's Progression in a Sex-Dependent Manner. Adv Sci (Weinh). 2024;11(9):e2306576. Epub 20231213. doi: 10.1002/advs.202306576. PubMed PMID: 38093507; PMCID: PMC10916590.
40. Arnold M, Nho K, Kueider-Paisley A, Massaro T, Huynh K, Brauner B, MahmoudianDehkordi S, Louie G, Moseley MA, Thompson JW, John-Williams LS, Tenenbaum JD, Blach C, Chang R, Brinton RD, Baillie R, Han X, Trojanowski JQ, Shaw LM, Martins R, Weiner MW, Trushina E, Toledo JB, Meikle PJ, Bennett DA, Krumsiek J, Doraiswamy PM, Saykin AJ, Kaddurah-Daouk R, Kastenmuller G. Sex and APOE epsilon4 genotype modify the Alzheimer's disease serum metabolome. Nat Commun. 2020;11(1):1148. Epub 20200302. doi: 10.1038/s41467-020-14959-w. PubMed PMID: 32123170; PMCID: PMC7052223.

41. Baloni P, Arnold M, Buitrago L, Nho K, Moreno H, Huynh K, Brauner B, Louie G, Kueider-Paisley A, Suhre K, Saykin AJ, Ekroos K, Meikle PJ, Hood L, Price ND, Alzheimer's Disease Metabolomics C, Doraiswamy PM, Funk CC, Hernandez AI, Kastenmuller G, Baillie R, Han X, Kaddurah-Daouk R. Multi-Omic analyses characterize the ceramide/sphingomyelin pathway as a therapeutic target in Alzheimer's disease. Commun Biol. 2022;5(1):1074. Epub 20221008. doi: 10.1038/s42003-022-04011-6. PubMed PMID: 36209301; PMCID: PMC9547905.
42. Liu Y, Thalamuthu A, Mather KA, Crawford J, Ulanova M, Wong MWK, Pickford R, Sachdev PS, Braidy N. Plasma lipidome is dysregulated in Alzheimer's disease and is associated with disease risk genes. Transl Psychiatry. 2021;11(1):344. Epub 20210607. doi: 10.1038/s41398-021-01362-2. PubMed PMID: 34092785; PMCID: PMC8180517.
43. Cutler RG, Kelly J, Storie K, Pedersen WA, Tammara A, Hatanpaa K, Troncoso JC, Mattson MP. Involvement of oxidative stress-induced abnormalities in ceramide and cholesterol metabolism in brain aging and Alzheimer's disease. Proc Natl Acad Sci U S A. 2004;101(7):2070–5. Epub 20040215. doi: 10.1073/pnas.0305799101. PubMed PMID: 14970312; PMCID: PMC357053.
44. Huynh K, Lim WLF, Giles C, Jayawardana KS, Salim A, Mellett NA, Smith AAT, Olshansky G, Drew BG, Chatterjee P, Martins I, Laws SM, Bush AI, Rowe CC, Villemagne VL, Ames D, Masters CL, Arnold M, Nho K, Saykin AJ, Baillie R, Han X, Kaddurah-Daouk R, Martins RN, Meikle PJ. Concordant peripheral lipidome signatures in two large clinical studies of Alzheimer's disease. Nat Commun. 2020;11(1):5698. Epub 20201110. doi: 10.1038/s41467-020-19473-7. PubMed PMID: 33173055; PMCID: PMC7655942.
45. Baloni P, Funk CC, Yan J, Yurkovich JT, Kueider-Paisley A, Nho K, Heinken A, Jia W, Mahmoudiandehkordi S, Louie G, Saykin AJ, Arnold M, Kastenmuller G, Griffiths WJ, Thiele I, Alzheimer's Disease Metabolomics C, Kaddurah-Daouk R, Price ND. Metabolic Network Analysis Reveals Altered Bile Acid Synthesis and Metabolism in Alzheimer's Disease. Cell Rep Med. 2020;1(8):100138. Epub 20201117. doi: 10.1016/j.xcrm.2020.100138. PubMed PMID: 33294859; PMCID: PMC7691449.
46. Greenberg N, Grassano A, Thambisetty M, Lovestone S, Legido-Quigley C. A proposed metabolic strategy for monitoring disease progression in Alzheimer's disease. Electrophoresis. 2009;30(7):1235–9. doi: 10.1002/elps.200800589. PubMed PMID: 19288586.
47. Lin W, Zhang J, Liu Y, Wu R, Yang H, Hu X, Ling X. Studies on diagnostic biomarkers and therapeutic mechanism of Alzheimer's disease through metabolomics and hippocampal proteomics. Eur J Pharm Sci. 2017;105:119–26. Epub 20170508. doi: 10.1016/j.ejps.2017.05.003. PubMed PMID: 28495476.
48. Kalecky K, German DC, Montillo AA, Bottiglieri T. Targeted Metabolomic Analysis in Alzheimer's Disease Plasma and Brain Tissue in Non-Hispanic Whites. J Alzheimers Dis. 2022;86(4):1875–95. doi: 10.3233/JAD-215448. PubMed PMID: 35253754; PMCID: PMC9108583.
49. Czech C, Berndt P, Busch K, Schmitz O, Wiemer J, Most V, Hampel H, Kastler J, Senn H. Metabolite profiling of Alzheimer's disease cerebrospinal fluid. PLoS One. 2012;7(2):e31501. Epub 20120216. doi: 10.1371/journal.pone.0031501. PubMed PMID: 22359596; PMCID: PMC3281064.
50. Buergel T, Steinfeldt J, Ruyoga G, Pietzner M, Bizzarri D, Vojinovic D, Upmeier Zu Belzen J, Loock L, Kittner P, Christmann L, Hollmann N, Strangalies H, Braunger JM, Wild B, Chiesa ST, Spranger J, Klostermann F, van den Akker EB, Trompet S, Mooijaart SP, Sattar N, Jukema JW, Lavrijssen B, Kavousi M, Ghanbari M, Ikram MA, Slagboom E, Kivimaki M, Langenberg C, Deanfield J, Eils R, Landmesser U. Metabolomic profiles predict individual multidisease outcomes. Nat Med. 2022;28(11):2309–20. Epub 20220922. doi: 10.1038/s41591-022-01980-3. PubMed PMID: 36138150; PMCID: PMC9671812.

51. Mak JKL, Kananen L, Qin C, Kuja-Halkola R, Tang B, Lin J, Wang Y, Jaaskelainen T, Koskinen S, Lu Y, Magnusson PKE, Hagg S, Jylhava J. Unraveling the metabolic underpinnings of frailty using multicohort observational and Mendelian randomization analyses. Aging Cell. 2023;22(8):e13868. Epub 20230515. doi: 10.1111/acel.13868. PubMed PMID: 37184129; PMCID: PMC10410014.
52. Low DY, Lefevre-Arbogast S, Gonzalez-Dominguez R, Urpi-Sarda M, Micheau P, Petera M, Centeno D, Durand S, Pujos-Guillot E, Korosi A, Lucassen PJ, Aigner L, Proust-Lima C, Hejblum BP, Helmer C, Andres-Lacueva C, Thuret S, Samieri C, Manach C. Diet-Related Metabolites Associated with Cognitive Decline Revealed by Untargeted Metabolomics in a Prospective Cohort. Mol Nutr Food Res. 2019;63(18):e1900177. Epub 20190709. doi: 10.1002/mnfr.201900177. PubMed PMID: 31218777; PMCID: PMC6790579.
53. Ticinesi A, Guerra A, Nouvenne A, Meschi T, Maggi S. Disentangling the Complexity of Nutrition, Frailty and Gut Microbial Pathways during Aging: A Focus on Hippuric Acid. Nutrients. 2023;15(5). Epub 20230224. doi: 10.3390/nu15051138. PubMed PMID: 36904138; PMCID: PMC10005077.
54. Rutledge GA, Sandhu AK, Miller MG, Edirisinghe I, Burton-Freeman BB, Shukitt-Hale B. Blueberry phenolics are associated with cognitive enhancement in supplemented healthy older adults. Food Funct. 2021;12(1):107–18. Epub 20201217. doi: 10.1039/d0fo02125c. PubMed PMID: 33331835.
55. He Y, Wang Y, Liu S, Pi Z, Liu Z, Xing J, Zhou H. A metabolomic study of the urine of rats with Alzheimer's disease and the efficacy of Ding-Zhi-Xiao-Wan on the afflicted rats. J Sep Sci. 2020;43(8):1458–65. Epub 20200226. doi: 10.1002/jssc.201900944. PubMed PMID: 32039552.
56. Klavins K, Koal T, Dallmann G, Marksteiner J, Kemmler G, Humpel C. The ratio of phosphatidylcholines to lysophosphatidylcholines in plasma differentiates healthy controls from patients with Alzheimer's disease and mild cognitive impairment. Alzheimers Dement (Amst). 2015;1(3):295–302. doi: 10.1016/j.dadm.2015.05.003. PubMed PMID: 26744734; PMCID: PMC4700585.
57. Whiley L, Sen A, Heaton J, Proitsi P, Garcia-Gomez D, Leung R, Smith N, Thambisetty M, Kloszewska I, Mecocci P, Soininen H, Tsolaki M, Vellas B, Lovestone S, Legido-Quigley C, AddNeuroMed C. Evidence of altered phosphatidylcholine metabolism in Alzheimer's disease. Neurobiol Aging. 2014;35(2):271–8. Epub 20130913. doi: 10.1016/j.neurobiolaging.2013.08.001. PubMed PMID: 24041970; PMCID: PMC5866043.
58. Arnold M, Buyukozkan M, Doraiswamy PM, Nho K, Wu T, Gudnason V, Launer LJ, Wang-Sattler R, Adamski J, Alzheimer's Disease Neuroimaging I, Alzheimer's Disease Metabolomics C, De Jager PL, Ertekin-Taner N, Bennett DA, Saykin AJ, Peters A, Suhre K, Kaddurah-Daouk R, Kastenmuller G, Krumsiek J. Individual bioenergetic capacity as a potential source of resilience to Alzheimer's disease. Nat Commun. 2025;16(1):1910. Epub 20250224. doi: 10.1038/s41467-025-57032-0. PubMed PMID: 39994231; PMCID: PMC11850607.
59. Sharmin T, Chatterjee P, Doecke JD, Ashton NJ, Huynh K, Pedrini S, Sohrabi HR, Heng B, Eslick S, Zetterberg H, Blennow K, Garg M, Martins RN. Circulating medium- and long-chain acylcarnitines are associated with plasma P-tau181 in cognitively normal older adults. J Neurochem. 2025;169(2). Epub 20241030. doi: 10.1111/jnc.16244. PubMed PMID: 39473263; PMCID: PMC11808462.
60. Heggermont WA, Papageorgiou AP, Heymans S, van Bilsen M. Metabolic support for the heart: complementary therapy for heart failure? Eur J Heart Fail. 2016;18(12):1420–9. Epub 20161104. doi: 10.1002/ejhf.678. PubMed PMID: 27813339.
61. Duran-Aniotz C, Hetz C. Glucose Metabolism: A Sweet Relief of Alzheimer's Disease. Curr Biol. 2016;26(17):R806–9. doi: 10.1016/j.cub.2016.07.060. PubMed PMID: 27623263.
62. Zhang X, Hu W, Wang Y, Wang W, Liao H, Zhang X, Kiburg KV, Shang X, Bulloch G, Huang Y, Zhang X, Tang S, Hu Y, Yu H, Yang X, He M, Zhu Z. Plasma metabolomic profiles of

dementia: a prospective study of 110,655 participants in the UK Biobank. BMC Med. 2022;20(1):252. Epub 20220815. doi: 10.1186/s12916-022-02449-3. PubMed PMID: 35965319; PMCID: PMC9377110.
63. Tynkkynen J, Chouraki V, van der Lee SJ, Hernesniemi J, Yang Q, Li S, Beiser A, Larson MG, Saaksjarvi K, Shipley MJ, Singh-Manoux A, Gerszten RE, Wang TJ, Havulinna AS, Wurtz P, Fischer K, Demirkan A, Ikram MA, Amin N, Lehtimaki T, Kahonen M, Perola M, Metspalu A, Kangas AJ, Soininen P, Ala-Korpela M, Vasan RS, Kivimaki M, van Duijn CM, Seshadri S, Salomaa V. Association of branched-chain amino acids and other circulating metabolites with risk of incident dementia and Alzheimer's disease: A prospective study in eight cohorts. Alzheimers Dement. 2018;14(6):723–33. Epub 20180306. doi: 10.1016/j.jalz.2018.01.003. PubMed PMID: 29519576; PMCID: PMC6082422.
64. Buondonno I, Sassi F, Carignano G, Dutto F, Ferreri C, Pili FG, Massaia M, Nisoli E, Ruocco C, Porrino P, Ravetta C, Riganti C, Isaia GC, D'Amelio P. From mitochondria to healthy aging: The role of branched-chain amino acids treatment: MATeR a randomized study. Clin Nutr. 2020;39(7):2080–91. Epub 20191018. doi: 10.1016/j.clnu.2019.10.013. PubMed PMID: 31672329.
65. Barazzoni R, Short KR, Nair KS. Effects of aging on mitochondrial DNA copy number and cytochrome c oxidase gene expression in rat skeletal muscle, liver, and heart. J Biol Chem. 2000;275(5):3343–7. doi: 10.1074/jbc.275.5.3343. PubMed PMID: 10652323.
66. Valerio A, D'Antona G, Nisoli E. Branched-chain amino acids, mitochondrial biogenesis, and healthspan: an evolutionary perspective. Aging (Albany NY). 2011;3(5):464–78. doi: 10.18632/aging.100322. PubMed PMID: 21566257; PMCID: PMC3156598.
67. Tan HC, Hsu JW, Kovalik JP, Eng A, Chan WH, Khoo CM, Tai ES, Chacko S, Jahoor F. Branched-Chain Amino Acid Oxidation Is Elevated in Adults with Morbid Obesity and Decreases Significantly after Sleeve Gastrectomy. J Nutr. 2020;150(12):3180–9. doi: 10.1093/jn/nxaa298. PubMed PMID: 33097955.
68. Vanweert F, de Ligt M, Hoeks J, Hesselink MKC, Schrauwen P, Phielix E. Elevated Plasma Branched-Chain Amino Acid Levels Correlate With Type 2 Diabetes-Related Metabolic Disturbances. J Clin Endocrinol Metab. 2021;106(4):e1827–e36. doi: 10.1210/clinem/dgaa751. PubMed PMID: 33079174.
69. Juricic P, Gronke S, Partridge L. Branched-Chain Amino Acids Have Equivalent Effects to Other Essential Amino Acids on Lifespan and Aging-Related Traits in Drosophila. J Gerontol A Biol Sci Med Sci. 2020;75(1):24–31. doi: 10.1093/gerona/glz080. PubMed PMID: 30891588; PMCID: PMC6909895.
70. Tramutola A, Triplett JC, Di Domenico F, Niedowicz DM, Murphy MP, Coccia R, Perluigi M, Butterfield DA. Alteration of mTOR signaling occurs early in the progression of Alzheimer disease (AD): analysis of brain from subjects with pre-clinical AD, amnestic mild cognitive impairment and late-stage AD. J Neurochem. 2015;133(5):739–49. Epub 20150226. doi: 10.1111/jnc.13037. PubMed PMID: 25645581.
71. Di Domenico F, Tramutola A, Foppoli C, Head E, Perluigi M, Butterfield DA. mTOR in Down syndrome: Role in Ass and tau neuropathology and transition to Alzheimer disease-like dementia. Free Radic Biol Med. 2018;114:94–101. Epub 20170812. doi: 10.1016/j.freeradbiomed.2017.08.009. PubMed PMID: 28807816; PMCID: PMC5748251.
72. Holecek M. Branched-chain amino acids in health and disease: metabolism, alterations in blood plasma, and as supplements. Nutr Metab (Lond). 2018;15(1):33. Epub 20180503. doi: 10.1186/s12986-018-0271-1. PubMed PMID: 29755574; PMCID: PMC5934885.
73. Judd JM, Jasbi P, Winslow W, Serrano GE, Beach TG, Klein-Seetharaman J, Velazquez R. Inflammation and the pathological progression of Alzheimer's disease are associated with low circulating choline levels. Acta Neuropathol. 2023;146(4):565–83. Epub 20230807. doi: 10.1007/s00401-023-02616-7. PubMed PMID: 37548694; PMCID: PMC10499952.

74. Lanari A, Amenta F, Silvestrelli G, Tomassoni D, Parnetti L. Neurotransmitter deficits in behavioural and psychological symptoms of Alzheimer's disease. Mech Ageing Dev. 2006;127(2):158–65. Epub 20051116. doi: 10.1016/j.mad.2005.09.016. PubMed PMID: 16297434.
75. DeLong CJ, Shen YJ, Thomas MJ, Cui Z. Molecular distinction of phosphatidylcholine synthesis between the CDP-choline pathway and phosphatidylethanolamine methylation pathway. J Biol Chem. 1999;274(42):29683–8. doi: 10.1074/jbc.274.42.29683. PubMed PMID: 10514439.
76. Allen DD, Smith QR. Characterization of the blood-brain barrier choline transporter using the in situ rat brain perfusion technique. J Neurochem. 2001;76(4):1032–41. doi: 10.1046/j.1471-4159.2001.00093.x. PubMed PMID: 11181822.
77. Wang R, Reddy PH. Role of Glutamate and NMDA Receptors in Alzheimer's Disease. J Alzheimers Dis. 2017;57(4):1041–8. doi: 10.3233/JAD-160763. PubMed PMID: 27662322; PMCID: PMC5791143.
78. Salcedo C, Andersen JV, Vinten KT, Pinborg LH, Waagepetersen HS, Freude KK, Aldana BI. Functional Metabolic Mapping Reveals Highly Active Branched-Chain Amino Acid Metabolism in Human Astrocytes, Which Is Impaired in iPSC-Derived Astrocytes in Alzheimer's Disease. Front Aging Neurosci. 2021;13:736580. Epub 20210917. doi: 10.3389/fnagi.2021.736580. PubMed PMID: 34603012; PMCID: PMC8484639.
79. Seshadri S, Beiser A, Selhub J, Jacques PF, Rosenberg IH, D'Agostino RB, Wilson PW, Wolf PA. Plasma homocysteine as a risk factor for dementia and Alzheimer's disease. N Engl J Med. 2002;346(7):476–83. doi: 10.1056/NEJMoa011613. PubMed PMID: 11844848.
80. Rahman ML, Shu XO, Jones DP, Hu W, Ji BT, Blechter B, Wong JYY, Cai Q, Yang G, Gao YT, Zheng W, Rothman N, Walker D, Lan Q. A nested case-control study of untargeted plasma metabolomics and lung cancer among never-smoking women within the prospective Shanghai Women's Health Study. Int J Cancer. 2024;155(3):508–18. Epub 20240423. doi: 10.1002/ijc.34929. PubMed PMID: 38651675; PMCID: PMC11284831.
81. Toyoshima K, Nakamura M, Adachi Y, Imaizumi A, Hakamada T, Abe Y, Kaneko E, Takahashi S, Shimokado K. Increased plasma proline concentrations are associated with sarcopenia in the elderly. PLoS One. 2017;12(9):e0185206. Epub 20170921. doi: 10.1371/journal.pone.0185206. PubMed PMID: 28934309; PMCID: PMC5608336.
82. Francois M, Karpe AV, Liu JW, Beale DJ, Hor M, Hecker J, Faunt J, Maddison J, Johns S, Doecke JD, Rose S, Leifert WR. Multi-Omics, an Integrated Approach to Identify Novel Blood Biomarkers of Alzheimer's Disease. Metabolites. 2022;12(10):949–. Epub 20221006. doi: 10.3390/metabo12100949. PubMed PMID: 36295851; PMCID: PMC9610280.
83. Corso G, Cristofano A, Sapere N, la Marca G, Angiolillo A, Vitale M, Fratangelo R, Lombardi T, Porcile C, Intrieri M, Di Costanzo A. Serum Amino Acid Profiles in Normal Subjects and in Patients with or at Risk of Alzheimer Dementia. Dement Geriatr Cogn Dis Extra. 2017;7(1):143–59. Epub 20170504. doi: 10.1159/000466688. PubMed PMID: 28626469; PMCID: PMC5471778.
84. Conde R, Oliveira N, Morais E, Amaral AP, Sousa A, Graca G, Verde I. NMR analysis seeking for cognitive decline and dementia metabolic markers in plasma from aged individuals. J Pharm Biomed Anal. 2024;238(115815):115815. Epub 20231027. doi: 10.1016/j.jpba.2023.115815. PubMed PMID: 37952448.
85. Chen T, Pan F, Huang Q, Xie G, Chao X, Wu L, Wang J, Cui L, Sun T, Li M, Wang Y, Guan Y, Zheng X, Ren Z, Guo Y, Wang L, Zhou K, Zhao A, Guo Q, Xie F, Jia W. Metabolic phenotyping reveals an emerging role of ammonia abnormality in Alzheimer's disease. Nat Commun. 2024;15(1):3796. Epub 20240507. doi: 10.1038/s41467-024-47897-y. PubMed PMID: 38714706; PMCID: PMC11076546.
86. Ren Z, Zhao L, Zhao M, Bao T, Chen T, Zhao A, Zheng X, Gu X, Sun T, Guo Y, Tang Y, Xie G, Jia W. Increased intestinal bile acid absorption contributes to age-related cognitive

impairment. Cell Rep Med. 2024;5(5):101543. Epub 20240501. doi: 10.1016/j.xcrm.2024.101543. PubMed PMID: 38697101; PMCID: PMC11148718.
87. Matsumoto S, Haberle J, Kido J, Mitsubuchi H, Endo F, Nakamura K. Urea cycle disorders-update. J Hum Genet. 2019;64(9):833–47. Epub 20190520. doi: 10.1038/s10038-019-0614-4. PubMed PMID: 31110235.
88. Liu P, Yang Q, Yu N, Cao Y, Wang X, Wang Z, Qiu WY, Ma C. Phenylalanine Metabolism Is Dysregulated in Human Hippocampus with Alzheimer's Disease Related Pathological Changes. J Alzheimers Dis. 2021;83(2):609–22. doi: 10.3233/JAD-210461. PubMed PMID: 34334403.
89. Cui M, Jiang Y, Zhao Q, Zhu Z, Liang X, Zhang K, Wu W, Dong Q, An Y, Tang H, Ding D, Chen X. Metabolomics and incident dementia in older Chinese adults: The Shanghai Aging Study. Alzheimers Dement. 2020;16(5):779–88. Epub 20200408. doi: 10.1002/alz.12074. PubMed PMID: 32270572.
90. Wang F, Wang G, Li W, Xu C, Zeng Z, Zhou Y. Analysis of serum metabolism in premature infants before and after feeding using GC-MS and the relationship with necrotizing enterocolitis. Biomed Chromatogr. 2023;37(1):e5505. Epub 20220925. doi: 10.1002/bmc.5505. PubMed PMID: 36093571; PMCID: PMC10078300.
91. Murtas G, Marcone GL, Sacchi S, Pollegioni L. L-serine synthesis via the phosphorylated pathway in humans. Cell Mol Life Sci. 2020;77(24):5131–48. Epub 20200627. doi: 10.1007/s00018-020-03574-z. PubMed PMID: 32594192; PMCID: PMC11105101.
92. Zhu Z, Shi Z, Xie C, Gong W, Hu Z, Peng Y. A novel mechanism of Gamma-aminobutyric acid (GABA) protecting human umbilical vein endothelial cells (HUVECs) against H(2)O(2)-induced oxidative injury. Comp Biochem Physiol C Toxicol Pharmacol. 2019;217:68–75. Epub 20181127. doi: 10.1016/j.cbpc.2018.11.018. PubMed PMID: 30500452.
93. Xu J, Green R, Kim M, Lord J, Ebshiana A, Westwood S, Baird AL, Nevado-Holgado AJ, Shi L, Hye A, Snowden SG, Bos I, Vos SJB, Vandenberghe R, Teunissen CE, Kate MT, Scheltens P, Gabel S, Meersmans K, Blin O, Richardson J, De Roeck EE, Engelborghs S, Sleegers K, Bordet R, Rami L, Kettunen P, Tsolaki M, Verhey FRJ, Alcolea D, Lleo A, Peyratout G, Tainta M, Johannsen P, Freund-Levi Y, Frolich L, Dobricic V, Frisoni GB, Molinuevo JL, Wallin A, Popp J, Martinez-Lage P, Bertram L, Blennow K, Zetterberg H, Streffer J, Visser PJ, Lovestone S, Proitsi P, Legido-Quigley C, On Behalf Of The European Medical Information Framework C. Sex-Specific Metabolic Pathways Were Associated with Alzheimer's Disease (AD) Endophenotypes in the European Medical Information Framework for AD Multimodal Biomarker Discovery Cohort. Biomedicines. 2021;9(11):1610–. Epub 20211103. doi: 10.3390/biomedicines9111610. PubMed PMID: 34829839; PMCID: PMC8615383.
94. Rebholz CM, Lichtenstein AH, Zheng Z, Appel LJ, Coresh J. Serum untargeted metabolomic profile of the Dietary Approaches to Stop Hypertension (DASH) dietary pattern. Am J Clin Nutr. 2018;108(2):243–55. doi: 10.1093/ajcn/nqy099. PubMed PMID: 29917038; PMCID: PMC6669331.
95. Chen H, Shen J, Tao Y, Zhang Y, Gao M, Ma Y, Zheng Y, Zong G, Lin Q, Tong L, Yuan C. Circulating metabolomic profile of the MIND diet and its relation to cognition in middle-aged and older adults. Alzheimer's & Dementia. 2025;20(S7). doi: 10.1002/alz.088163.
96. Zhan M, Li Z, Chen J, Zhao Y, Bai Z, Lu B, Chen H, Liu Y. Indoxyl sulfate (IS) mediates pro-inflammatory responses in severe pneumonia in patients with rheumatoid arthritis associated interstitial lung disease. Clin Immunol. 2025;272(110430):110430. Epub 20250126. doi: 10.1016/j.clim.2025.110430. PubMed PMID: 39875062.
97. Stepanova N, Driianska V, Korol L, Snisar L. Association between serum total indoxyl sulfate, intraperitoneal inflammation, and peritoneal dialysis technique failure: a 3-year prospective cohort study. BMC Nephrol. 2024;25(1):475. Epub 20241231. doi: 10.1186/s12882-024-03935-x. PubMed PMID: 39741261; PMCID: PMC11689590.

98. Hendrikx T, Schnabl B. Indoles: metabolites produced by intestinal bacteria capable of controlling liver disease manifestation. J Intern Med. 2019;286(1):32–40. Epub 20190314. doi: 10.1111/joim.12892. PubMed PMID: 30873652.
99. Bendheim PE, Poeggeler B, Neria E, Ziv V, Pappolla MA, Chain DG. Development of indole-3-propionic acid (OXIGON) for Alzheimer's disease. J Mol Neurosci. 2002;19(1-2):213–7. doi: 10.1007/s12031-002-0036-0. PubMed PMID: 12212784.
100. Pappolla MA, Perry G, Fang X, Zagorski M, Sambamurti K, Poeggeler B. Indoles as essential mediators in the gut-brain axis. Their role in Alzheimer's disease. Neurobiol Dis. 2021;156:105403. Epub 20210601. doi: 10.1016/j.nbd.2021.105403. PubMed PMID: 34087380.
101. Sathyasaikumar KV, Blanco-Ayala T, Zheng Y, Schwieler L, Erhardt S, Tufvesson-Alm M, Poeggeler B, Schwarcz R. The Tryptophan Metabolite Indole-3-Propionic Acid Raises Kynurenic Acid Levels in the Rat Brain In Vivo. Int J Tryptophan Res. 2024;17:11786469241262876. Epub 20240620. doi: 10.1177/11786469241262876. PubMed PMID: 38911967; PMCID: PMC11191616.
102. Ma YY, Li X, Yu JT, Wang YJ. Therapeutics for neurodegenerative diseases by targeting the gut microbiome: from bench to bedside. Transl Neurodegener. 2024;13(1):12. Epub 20240227. doi: 10.1186/s40035-024-00404-1. PubMed PMID: 38414054; PMCID: PMC10898075.
103. Feliers D, Lee DY, Gorin Y, Kasinath BS. Symmetric dimethylarginine alters endothelial nitric oxide activity in glomerular endothelial cells. Cell Signal. 2015;27(1):1–5. Epub 20141008. doi: 10.1016/j.cellsig.2014.09.024. PubMed PMID: 25283600.
104. Tyagi N, Sedoris KC, Steed M, Ovechkin AV, Moshal KS, Tyagi SC. Mechanisms of homocysteine-induced oxidative stress. Am J Physiol Heart Circ Physiol. 2005;289(6):H2649–56. Epub 20050805. doi: 10.1152/ajpheart.00548.2005. PubMed PMID: 16085680.
105. Gokkusu C, Tulubas F, Unlucerci Y, Ozkok E, Umman B, Aydin M. Homocysteine and pro-inflammatory cytokine concentrations in acute heart disease. Cytokine. 2010;50(1):15–8. Epub 20100202. doi: 10.1016/j.cyto.2009.12.015. PubMed PMID: 20129796.
106. Smith AD, Refsum H, Bottiglieri T, Fenech M, Hooshmand B, McCaddon A, Miller JW, Rosenberg IH, Obeid R. Homocysteine and Dementia: An International Consensus Statement. J Alzheimers Dis. 2018;62(2):561–70. doi: 10.3233/JAD-171042. PubMed PMID: 29480200; PMCID: PMC5836397.
107. Braissant O. Ammonia toxicity to the brain: effects on creatine metabolism and transport and protective roles of creatine. Mol Genet Metab. 2010;100 Suppl 1:S53–8. Epub 20100214. doi: 10.1016/j.ymgme.2010.02.011. PubMed PMID: 20227315.
108. Butterfield DA, Hensley K, Cole P, Subramaniam R, Aksenov M, Aksenova M, Bummer PM, Haley BE, Carney JM. Oxidatively induced structural alteration of glutamine synthetase assessed by analysis of spin label incorporation kinetics: relevance to Alzheimer's disease. J Neurochem. 1997;68(6):2451–7. doi: 10.1046/j.1471-4159.1997.68062451.x. PubMed PMID: 9166739.
109. Moreira P, Honda K, Liu Q, Aliev G, Oliveira C, Santos M, Zhu X, Smith M, Perry G. Alzheimers Disease and Oxidative Stress: The Old Problem Remains Unsolved. Current Medicinal Chemistry-Central Nervous System Agents. 2005;5(1):51–62. doi: 10.2174/1568015053202714.
110. Rehman T, Shabbir MA, Inam-Ur-Raheem M, Manzoor MF, Ahmad N, Liu ZW, Ahmad MH, Siddeeg A, Abid M, Aadil RM. Cysteine and homocysteine as biomarker of various diseases. Food Sci Nutr. 2020;8(9):4696–707. Epub 20200812. doi: 10.1002/fsn3.1818. PubMed PMID: 32994931; PMCID: PMC7500767.
111. Ezerina D, Takano Y, Hanaoka K, Urano Y, Dick TP. N-Acetyl Cysteine Functions as a Fast-Acting Antioxidant by Triggering Intracellular H(2)S and Sulfane Sulfur Production. Cell Chem Biol. 2018;25(4):447–59 e4. Epub 20180208. doi: 10.1016/j.chembiol.2018.01.011. PubMed PMID: 29429900; PMCID: PMC6455997.

112. Le Chatelier E, Nielsen T, Qin J, Prifti E, Hildebrand F, Falony G, Almeida M, Arumugam M, Batto JM, Kennedy S, Leonard P, Li J, Burgdorf K, Grarup N, Jorgensen T, Brandslund I, Nielsen HB, Juncker AS, Bertalan M, Levenez F, Pons N, Rasmussen S, Sunagawa S, Tap J, Tims S, Zoetendal EG, Brunak S, Clement K, Dore J, Kleerebezem M, Kristiansen K, Renault P, Sicheritz-Ponten T, de Vos WM, Zucker JD, Raes J, Hansen T, Meta HITc, Bork P, Wang J, Ehrlich SD, Pedersen O. Richness of human gut microbiome correlates with metabolic markers. Nature. 2013;500(7464):541–6. doi: 10.1038/nature12506. PubMed PMID: 23985870.
113. Bell LK, Edwards S, Grieger JA. The Relationship between Dietary Patterns and Metabolic Health in a Representative Sample of Adult Australians. Nutrients. 2015;7(8):6491–505. Epub 20150805. doi: 10.3390/nu7085295. PubMed PMID: 26251918; PMCID: PMC4555134.

a Study design

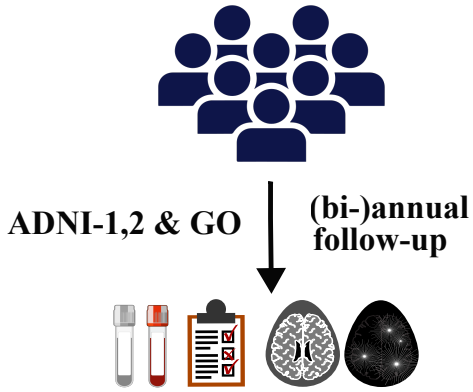

b Data acquistion & QC

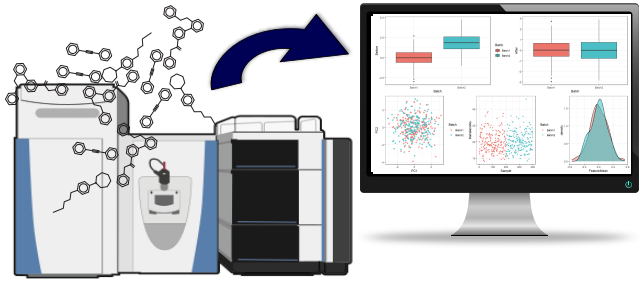

Post QC - 4063 samples from 1430 individuals and 506 metabolites

c Medication selection

d Statistical analysis

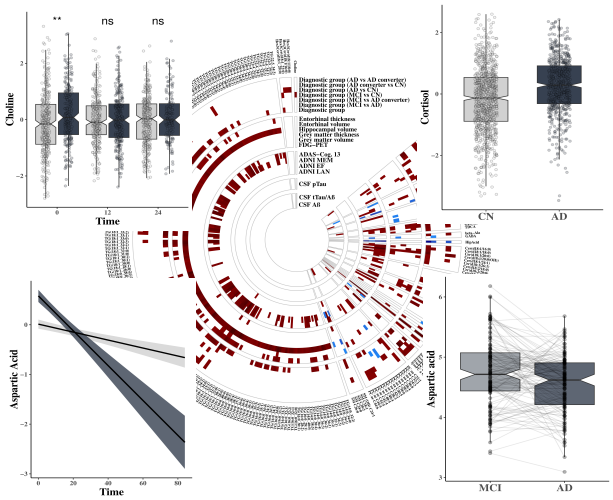

e Association patterns

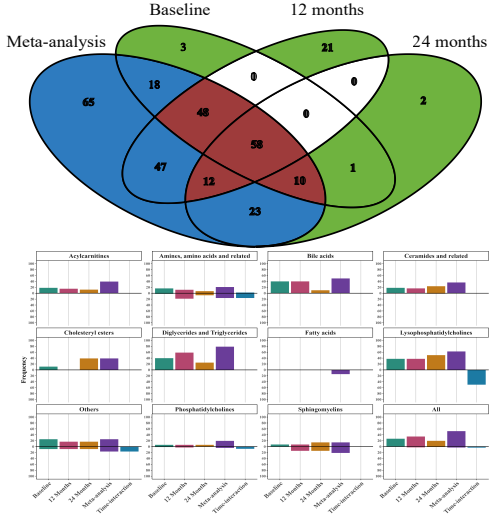

f Interactive app

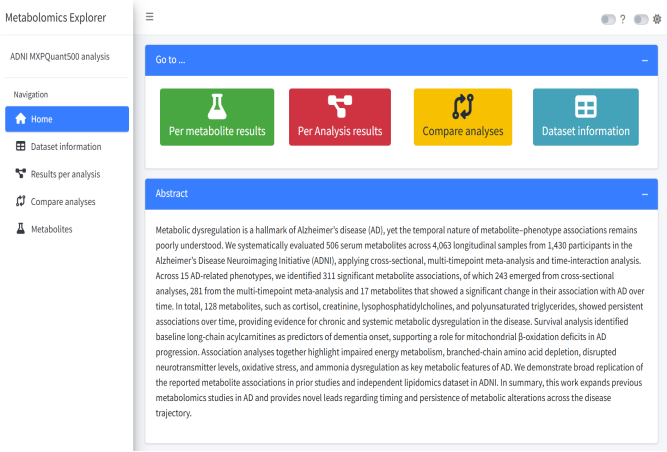

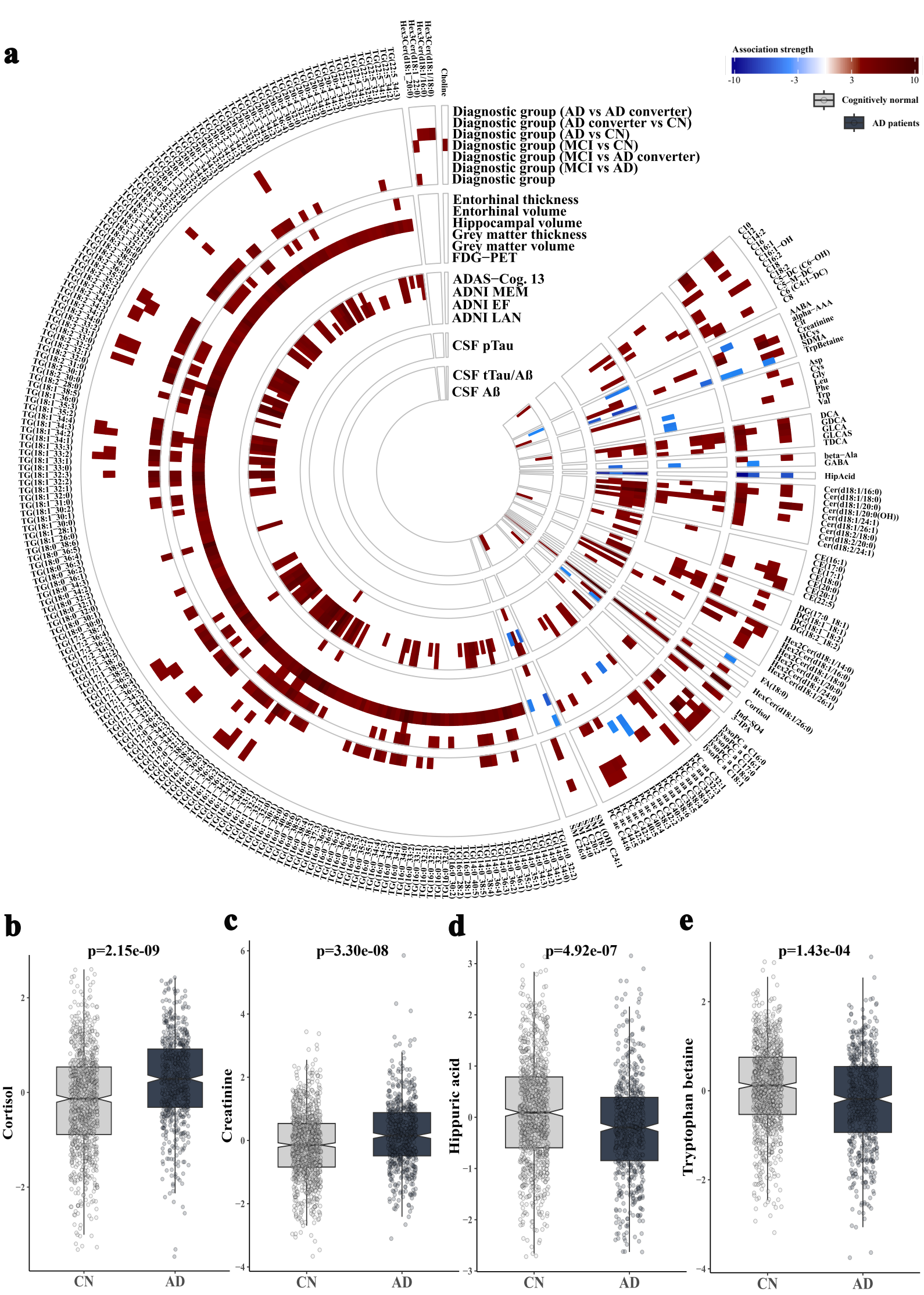
a
Association strength
-10
-3
3
10
Cognitively normal
AD patients
Choline
Diagnostic group (AD vs AD converter)
Diagnostic group (AD converter vs CN)
Diagnostic group (AD vs CN)
Diagnostic group (MCI vs CN)
Diagnostic group (MCI vs AD converter)
Diagnostic group (MCI vs AD)
Diagnostic group
Entorhinal thickness
Entorhinal volume
Hippocampal volume
Grey matter thickness
Grey matter volume
FDG−PET
ADAS−Cog. 13
ADNI MEM
ADNI EF
ADNI LAN
CSF pTau
CSF tTau/Aß
CSF Aß
b
p=2.15e-09
Cortisol
CN
AD
c
p=3.30e-08
Creatinine
CN
AD
d
p=4.92e-07
Hippuric acid
CN
AD
e
p=1.43e-04
Tryptophan betaine
CN
AD

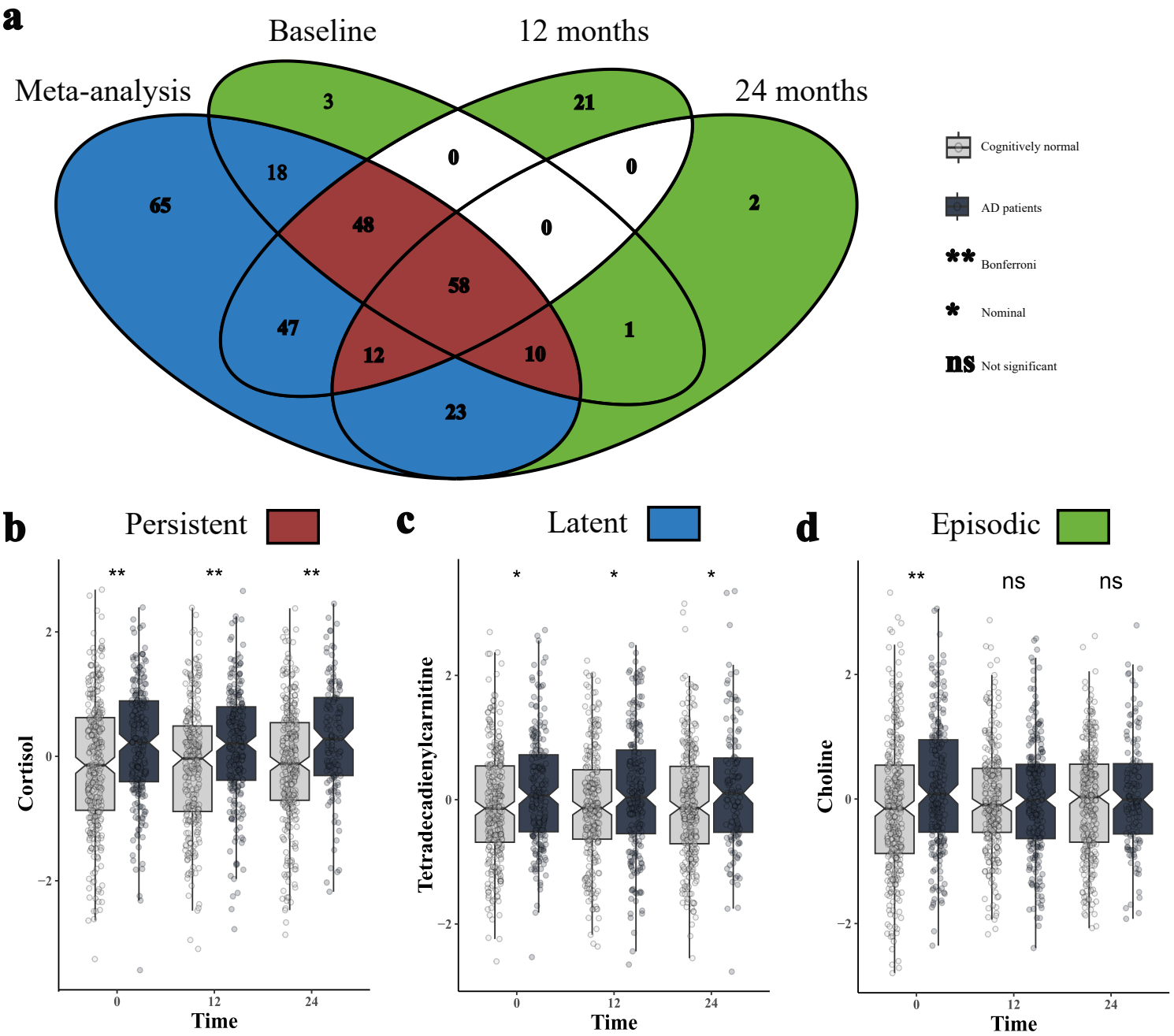
a
Baseline
12 months
Meta-analysis
24 months
3
21
0
0
18
65
48
0
2
58
47
1
12
10
23
Cognitively normal
AD patients
** Bonferroni
* Nominal
ns Not significant
b
Persistent
c
Latent
d
Episodic
Cortisol
Tetradecadienylcarnitine
Choline
Time
**
*
ns

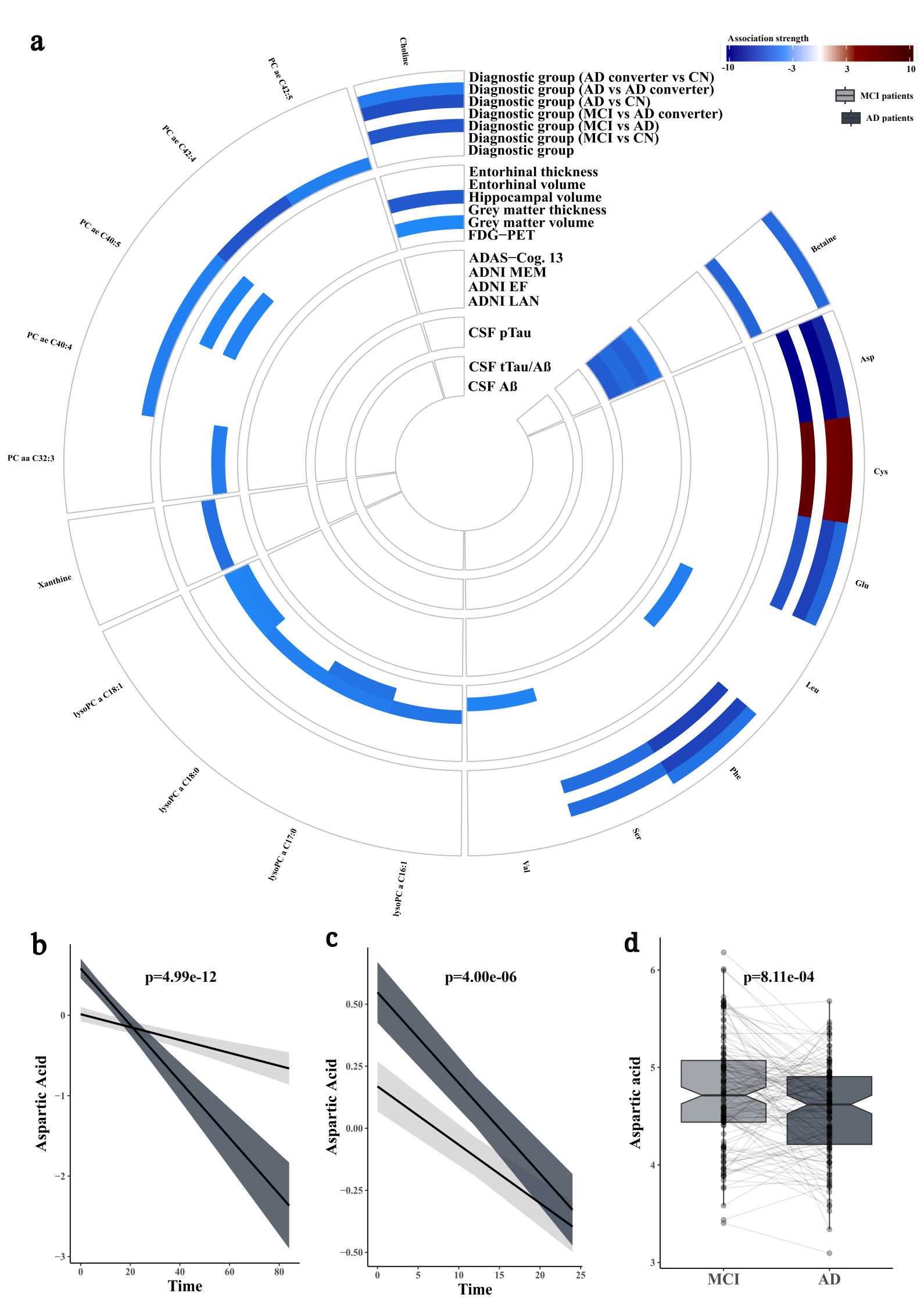
a
Association strength
-10
-3
3
10
MCI patients
AD patients
Diagnostic group (AD converter vs CN)
Diagnostic group (AD vs AD converter)
Diagnostic group (AD vs CN)
Diagnostic group (MCI vs AD converter)
Diagnostic group (MCI vs AD)
Diagnostic group (MCI vs CN)
Diagnostic group
Entorhinal thickness
Entorhinal volume
Hippocampal volume
Grey matter thickness
Grey matter volume
FDG−PET
ADAS−Cog. 13
ADNI MEM
ADNI EF
ADNI LAN
CSF pTau
CSF tTau/Aß
CSF Aß
Choline
PC ae C42:5
PC ae C42:4
PC ae C40:5
PC ae C40:4
PC aa C32:3
Xanthine
lysoPC a C18:1
lysoPC a C18:0
lysoPC a C17:0
lysoPC a C16:1
Val
Ser
Phe
Leu
Glu
Cys
Asp
Betaine
b
p=4.99e-12
Aspartic Acid
Time
c
p=4.00e-06
Aspartic Acid
Time
d
p=8.11e-04
Aspartic acid
MCI
AD

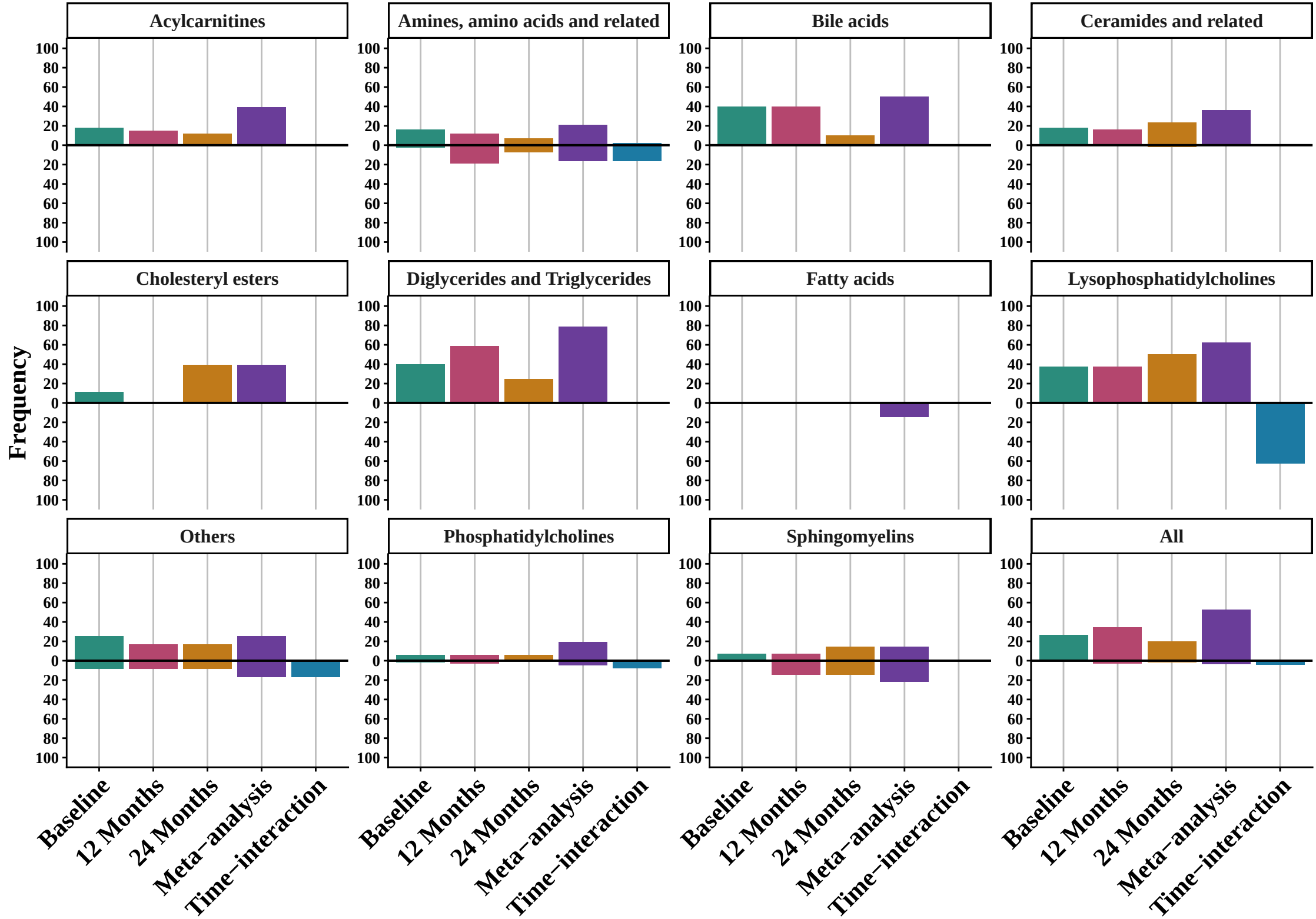
Acylcarnitines
Amines, amino acids and related
Bile acids
Ceramides and related
Cholesteryl esters
Diglycerides and Triglycerides
Fatty acids
Lysophosphatidylcholines
Others
Phosphatidylcholines
Sphingomyelins
All
Frequency
100
80
60
40
20
0
20
40
60
80
100
Baseline
12 Months
24 Months
Meta−analysis
Time−interaction